2
mix

X-621-73-106

PREPRINT

NASA TM X- 66234

FULL NON-LINEAR TREATMENT OF THE GLOBAL THERMOSPHERIC WIND SYSTEM

PART 2: RESULTS AND COMPARISON WITH OBSERVATIONS

P. W. BLUM
I. HARRIS

GODDARD SPACE FLIGHT CENTER
GREENBELT, MARYLAND

X-621-73-106

FULL NON-LINEAR TREATMENT OF THE GLOBAL THERMOSPHERIC WIND SYSTEM

PART 2: RESULTS AND COMPARISON WITH OBSERVATIONS

P. W. Blum

and

I. Harris

April 1973

GODDARD SPACE FLIGHT CENTER

Greenbelt, Maryland

CONTENTS

FULL NON-LINEAR TREATMENT OF THE GLOBAL THERMOSPHERIC WIND SYSTEM

PART 2: RESULTS AND COMPARISONS WITH OBSERVATIONS

INTRODUCTION

Part 1 has outlined the mathematical method used in the integration of the equations describing the global thermospheric motions and detailed the empirical models of the driving forces and the drag forces which were used. In this part the resulting global pattern of winds is described. Considered here are the effects of the inclusion of the non-linear parts of the convective derivative on the resulting wind pattern. A comparison is made with earlier theoretical work and with winds deduced from observations.

When reference is made to equations or figures from part 1, these references are prefixed with 1.

DESCRIPTION OF THE WIND FIELD

The global pattern of the thermospheric winds at a height of 300 km is shown in Figure 1 for equinox and Figures 2 and 3 for solstice conditions. At the poles the zonal and the meridional velocities are related kinematically, as shown in part 1. The wind at the poles blows from the day side at about 13 hours L. T. (local time) toward the night side at about 1 hour L. T. The magnitude of the velocity is approximately 100 m/sec.

The zonal winds have their maximum in the eastward direction close to 20 hour L. T. with little dependence of the time of the maximum wind on latitude. The amplitude of the zonal winds in the isothermal region is between 70 to 130 m/sec, depending upon latitude. The diurnal average zonal wind is also latitudinally dependent-having an eastward direction at almost all latitudes at equinox. The average, i. e., the diurnal mean velocity, is about 2 to 18 m/sec above 300 km at equinox (Figure 4). As the average zonal pressure gradient is nearly zero, this small flow is due to the variation of ion drag with local time.

At solstice conditions the latitudinal variation of the mean zonal flow is considerable. In the summer hemisphere it is generally westwards with a velocity of 2 to 15 m/sec; in the winter hemisphere it is eastwards with a velocity up to 50 m/sec. King-Hele (1970), has found a mean eastward flow in the equatorial regions of about 45- 70 m/sec. Our calculations do not result in mean eastward velocities of this magnitude. We also cannot confirm Chiu's (1971) contention that the superrotation is a non-linear effect as a comparison between our linear and non-linear solutions does not show any difference between the mean zonal velocities to any significant extent.

The meridional winds have a non-zero time-independent (diurnal mean) component that is strongly dependent on latitude and season. For equinox conditions the amplitude of the time-independent, the diurnal and the semi-diurnal components are shown in Figure 5. The time-independent component is directed towards the equator at equinox for both hemispheres but is southward during summer and northwards during winter at most latitudes as can be seen from Figure 6. The diurnal component of the meridional winds has a maximum between midnight and 1 hour L. T. except in the equatorial zone. The latitudinal dependence of its time of maximum is shown in Figure 7. The time dependence of the meridional winds for several latitudes is shown in Figure 8 for equinox and Figure 9 for solstice conditions.

The altitude dependence of both meridional and zonal winds is irregular below 250 km, and no great physical significance should be attached to it. Above 400 km the altitude dependent variation of the winds becomes small due to the influence of viscocity: it is less than 10%. This is demonstrated in Figures 10 and 11 for the zonal velocities.

VARIATIONS OF THE WIND SYSTEM WITH SOLAR ACTIVITY

Most of our model calculations were carried out for a solar activity of $F_{10.7} = 200$, and all figures and diagrams in this paper refer to this level of solar activity unless otherwise indicated. The driving forces are nearly independent of solar activity, but the ion densities increase markedly with increasing solar activity and the ion drag increases proportionally. As a first approximation this results in wind amplitudes that are inversely proportional to solar activity.

This was borne out by our calculations with solar activities less than 200. Cho and Yeh have also found large velocities at low solar activities (Cho and Yeh, 1970). Unfortunately, as the ion drag becomes smaller and the amplitude of the velocities higher, the convergence of our non-linear iteration scheme becomes difficult: at too low levels of solar activity (below $F_{10.7} = 100$) the scheme diverges, especially during solstice conditions. The divergence is mainly due to the very high velocities of the linear solution that are used as an initial guess for the iteration scheme. At mid-latitudes the initial velocities are larger than the local rotational velocity of the earth and therefore a divergence according to Kallina's (1970) theorem may occur. An improved iteration scheme could probably remedy the problem. An example of the dependence of the zonal velocities on solar activity is seen in Figure 11.

EFFECT OF LOWER BOUNDARY CONDITIONS

It was already mentioned that the effect of a non-zero velocity at the 120 km level will be unimportant for the velocities in the isothermal region due to the relatively low value of the kinematic viscocity at 120 km. In order to estimate accurately the effect of a non-vanishing velocity distribution at the lower boundary a test calculation was performed. It was assumed that at 120 km there exists a velocity distribution given by

$$V(\theta) = 0; \quad V(\phi) = 100 \sin \theta \ \text{m/sec}$$

This boundary condition is equivalent to a rotation of the atmosphere with a velocity of 100 m/sec in excess of the rotational velocity of the earth. The resulting height profile of the velocities, both zonal and meridional, is shown in Figure 12. All the non-linear terms were included in the test computation. It is seen that above a height of 200 km the effect of the lower boundary is negligible. This is also in accordance with the observations of rapid velocity shears between 100 and 160 km as observed by Smith (1972). Such shears would not be possible if the viscous drag in this height region were not small. As we claim physical meaningfulness of the computed wind field only at heights above 180 km, possibly even only 250 km, the test calculation shows that our results are not sensitive to the lower boundary conditions.

ACCURACY OF THE CALCULATED WIND PATTERN

Deviations between our computed results and the physical wind field may arise due to a variety of reasons:

1. The inaccuracy of the pressure gradients as determined from the Jacchia model.
2. Especially the higher Fourier modes are not included in the Jacchia model, and, therefore, no variations of the wind field with characteristic times of less than 6 hours can be obtained by employing driving forces derived from the Jacchia model.
3. The meridional pressure gradients as deduced from the Jacchia model are also open to question. Relatively minor changes of the latitudinal density and temperature dependence would cause considerable changes in the meridional pressure gradients. A demonstration of this effect will be given later.

4. The longitudinal averaging of the ion densities will have a smoothing effect on the computed winds.
5. The neglect of meridional electric fields may cause the zonal velocity to be slightly in error.
6. The cut-off of the higher Fourier modes of the ion distribution may introduce errors at local times close to sunrise and sunset.
7. In regions were the meridional velocity gradients are large our finite difference scheme can introduce truncation errors. Our solutions are always very good solutions of the system of difference equations which represent the non-linear differential equations. The residues of our solutions of the difference equations are less than 0.5% of the magnitude of the main terms appearing in the equations. The residues could be further decreased, but such a decrease would only change the solutions insignificantly. On the other hand, in regions of large velocity gradients the solution of the difference equations may not be a good approximation of the solution of the non-linear differential equations, as the mesh size may not be small enough. In such a region there is a possibility that our solutions differ from the true solutions of the differential equations. For this reason at equinox between 10° and -10° latitude and at solstice in the equatorial regions the accuracy of our solutions is somewhat reduced. The decreased accuracy may affect the phase and the amplitudes of the deduced winds in the equatorial zone.

TREATMENT OF THE NON-LINEAR TERMS IN EARLIER INVESTIGATIONS

The non-linear terms of the convective derivative represent part of the inertia of the flowing gas. They express the influence of the flow of the gas on neighbouring regions. Thus, it is to be expected that the major effect of the non-linear terms is to smooth out the effects of sudden changes of the pressure gradients or the drag forces on the velocities. Calculations ignoring the non-linear terms must be understood as yielding the flow of the gas at a given geographical position without the consideration of the velocity distribution at neighboring points, both in the zonal and the meridional directions. The magnitude of the non-linear terms will depend upon the velocity gradients that exist. In our formulation the magnitude of the zonal velocity gradients relative to the linear inertial term can be easily estimated as for the k-th harmonic component it is equal to k times the ratio of the flow velocity to the earth's rotational velocity ω r. However, meridional gradients are more difficult to estimate without explicit calculations. Non-linear terms have been partially included in previous calculations by considering the terms involving the east-west derivatives but neglecting the meridional coupling of the velocities.

Geisler (1967) has estimated the magnitude of the non-linear terms related to the zonal derivatives and concludes that these may have an appreciable influence on the wind field. Bailey et al. (1968) also estimate the non-linear terms for both the zonal and the meridional derivatives at mid-latitudes and find that these terms may at certain local times be of considerable magnitude. Stubbe

(1970) has included the zonal non-linear terms in his solution of the coupled heat conduction equation, continuity equations for ions and neutral particles and horizontal equations of motion. He states that the zonal gradients affect the results by about 10%. Rüster and Dudeney (1971) investigated the effects of the non-linear terms at mid-latitudes, but in common with all other previous work both Rüster et al. and Stubbe did not include latitudinal coupling. As Rüster et al. deal specifically with the non-linear effects, we will discuss their results in more detail. They have included the zonal derivatives and from the results obtained estimated the meridional derivatives but have not iterated the calculations using revised values for the inertial terms arising from the meridional gradients. Furthermore, they restricted themselves to one particular geographic position at a latitude of 45° S and a longitude of 55° W. This particular location was chosen because there the geomagnetic declination D vanishes and local time and zonal derivatives could be interchanged. In this context it should be remarked that the condition $D = 0$ is not required for the interchangability of these two derivatives. It is rather the condition $\partial D/\partial\lambda = 0$, that assures the interchangability; i.e., no changes of magnetic declination with longitude should occur. When the declination has a non-zero value, the expression for the ion drag (1.42) still holds, but its resolution into meridional and zonal components is not as simple as given by (1.42). Therefore, the more complicated expressions of Cho and Yeh (1970) must be used. Although the solution for the time-variation of the wind field will be periodic at a given geographical position for all geomagnetic declinations, the interchange of the longitudinal and time derivatives of the velocity requires the condition $\partial D/\partial\lambda = 0$. At the geographic location which Rüster et al. have chosen, they find that the inclusion of the non-linear terms causes a slight increase in the magnitude of the winds and an advance in phase of the winds in the early morning hours by about one hour as compared to their linear solution. Our results do not confirm this: we find at mid-latitudes a decrease of all Fourier components of the winds by about 5 to 8% and no appreciable change in the phase of the winds when our linear and full non-linear results are compared. In common with Stubbe and Rüster et al. we also found that the non-linear terms at mid-latitudes affect the winds by 10% or less. Only in the equatorial zones, as will be shown later, are the effects of the non-linearities much larger.

Rishbeth (1971 and 1972) finds that the non-linear terms mainly affect the phase of the winds at sunrise. We would like to qualify this statement and limit it to mid-latitudes and consideration of the zonal non-linear terms only.

COMPARISON OF LINEAR AND NON-LINEAR SOLUTION

As stated, we would expect generally a non-linear solution to have a smoother wind pattern, especially when the latitudinal dependence is considered, but our results do not fully confirm this. Possible rapid longitudinal variations of the wind field that may exist are smoothed in our computation by the limited number of Fourier terms that are considered. Steep local time or longitudinal velocity gradients would require for their description higher Fourier terms. The mesh size in latitude of our system of finite difference equations puts a limit on the variation of the velocity gradients in the meridional direction, as obviously the number of nodes is limited by the number of latitudinal meshpoints. This is similar to the limitation imposed on the gradients in the zonal direction by the number of Fourier terms. By including only the Fourier coefficients up to the semi-diurnal mode, we have effectively reduced the velocity gradients in the azimuthal direction to a rather low level. The justification for the exclusion of the higher Fourier modes is to be seen in the density model of Jacchia which does not include Fourier terms of higher order than 2 to any appreciable extent. On the other hand, the rapid changes of ion density near sunrise and sunset indicate that the ion drag term includes higher order harmonics. As these have not been included in our model, the possibility that such rapid ion drag variations would also have resulted in strong velocity gradients in the azimuthal direction should not be rejected outrightly. On the other hand, the computations of Rüster and Dudeney (1972) who have not used Fourier-analysis and therefore included effectively Fourier components of high order do not indicate that such is the case.

For these reasons the non-linear terms in our calculation will affect mainly the velocity gradients in the meridional direction. We shall discuss these briefly. The zonal velocities show only a small meridional variation because the pressure gradients of the Jacchia model depend little on latitude as shown in Figure 1.5. At equinox conditions the meridional winds have small meridional gradients. Therefore, the influence of the non-linear terms on the solution of the equations of motion is not very significant. In fact, Figure 5 shows that at a latitude of 30° there is almost no difference between the linear and the non-linear solutions, though at higher latitudes there is some difference. At the equator the meridional winds are zero at equinox for both the linear and the non-linear solutions. The differences between the linear and non-linear solutions are mainly to be found between the latitudes of 30° N and 30° S. Figure 13 shows the linear and non-linear solutions at equinox for the time-dependence of the meridional winds at latitudes of 10° and 30°. At solstice conditions the vanishing of the ion drag in the meridional direction near the geomagnetic equator causes large meridional velocities unless the driving forces vanish also at the equator. This is not the case with the Jacchia model for the diurnal average Fourier coefficient of the driving force during solstice conditions, though it occurs at equinoxes.

A complete vanishing of the ion drag force in the meridional direction at the equator would cause a singularity of the linear equations similar to the situation at the critical latitudes of tidal theory (Brillouin, 1932). For solstice conditions the latitudinal dependence of the average meridional velocity of the linear and non-linear solution is shown in Figure 6. The local time dependence of the meridional winds for the linear and non-linear solutions is shown for several latitudes in Figures 14 and 15. The amplitude and phase of the diurnal component of the meridional winds at solstice are compared for the linear and non-linear solutions in Figure 16.

In the case of solstice conditions and with the driving forces, according to the Jacchia model, the solution of the full non-linear set of equations (1.4) provides the only reasonable approach. It is not without cause that previous investigations have avoided the treatment of the equatorial regions at solstice conditions, or at least have not included the time-independent part of the meridional pressure gradients that are derived from Jacchia's model. At the equator the Coriolis force vanishes, and the equation for the meridional velocity becomes simply (after division by ω)

$$\frac{1}{\omega}\frac{DV^{(\theta)}}{Dt} + D_{ion}^{(\theta)} V^{(\theta)} - \eta \frac{\partial^2 V^{(\theta)}}{\partial z^2} = f_d^{(\theta)} \tag{2.1}$$

The meridional ion drag coefficient D_{ion} at the equator vanishes if we assume an aligned dipole geomagnetic field; the coefficient becomes small when geomagnetic declination effects are taken into account. A crude way to estimate the effect of the viscocity term $\eta\ \partial^2 V^{(\theta)}/\partial z^2$ is to take account of the height independence of the velocities above 300 km and solve equation (2.1) for parameters and variables averaged over the height range between 300 and 500 km.

Our equation then becomes

$$\frac{1}{\omega}\frac{D\overline{V}^{(\theta)}}{Dt} + \overline{D}_{ion}^{(\theta)} \overline{V}^{(\theta)} = \overline{f}_d^{(\theta)} \tag{2.2}$$

and if we linearize the convective derivative simply

$$\frac{1}{\omega}\frac{\partial\overline{V}^{(\theta)}}{\partial t} + \overline{D}_{ion}^{(\theta)} \overline{V}^{(\theta)} = \overline{f}_d^{(\theta)} \tag{2.3}$$

On Fourier separation of the above equation the time independent meridional velocity is given by

$$\overline{V}_o^{(\theta)} = \overline{f}_d^{(\theta)}/D_{ion}^{(\theta)} \tag{2.3}$$

As D_{ion} is very small and $\overline{f}_d^{(\theta)}$ as deduced from the Jacchia model about 250 m/sec (Figure 1.6), the time-independent meridional wind component that results is nearly 700 m/sec. This result deviates grossly from the true state of the thermosphere. We cannot avoid this difficulty by solving equation (2.3) by an iteration scheme until the solution becomes periodic, as the results are not changed by the method of solution. We also have investigated equation (2.3) with the viscous term included and found that the solution becomes very sensitive to the upper boundary conditions, i.e., the exact altitude at which $\partial V/\partial z = 0$ is assumed. Therefore, the proper treatment of the problem in the equatorial region during solstice conditions must include the non-linear terms in the convective derivative of the meridional flow and also possibly the viscous drag. Solutions of the linearized equations of motion for the equatorial regions should be viewed with caution.

COMPARISON WITH EARLIER THEORETICAL WORK

Various authors have previously computed the thermospheric neutral winds. Although methods and conditions for which these calculations have been performed differ, a comparison will be made with the results presented here. The calculations by Geisler (1967) are similar in scope to ours as he also presents a global model of the wind pattern. Geisler calculates the pressure gradients from an unmodified Jacchia model for equinox conditions assumes a simple model of ion distribution: one profile for daytime and another for nighttime with no variations with latitude.

The zonal winds in Geisler's calculation peak about sunset with a small westward component for the diurnal mean zonal wind. Our calculations have shown a peak of the zonal velocity at about 20 hours L. T. with a mean value of about 10 m/sec towards the east at mid- and low latitudes. This difference may be ascribed to the difference in the treatment of the ion drag. Geisler's meridional winds change from a southward to a northward direction in the northern hemisphere at successively later times in the morning hours as the latitude decreases. This is similar to the behavior deduced by us (Figure 8). The transition from a southward to a northward wind is not as sharply defined in our calculation as in Geisler's, especially at high latitudes. This again may be due to the treatment of the ion drag as an ion distribution, as used by Geisler, with one value during the day and another during the night will have no semi-diurnal component, though higher Fourier modes are present.

The calculation of Kohl and King (1967) was performed for equinox conditions at a medium level of solar activity with a local time and latitude independent ion distribution. Furthermore, the form of the driving force used in the calculation, although based on the Jacchia model, included only a diurnal component. Both the average and the semi-diurnal components were neglected.

Thus, a global model of winds results that has only diurnal components for both the meridional and the zonal winds. Another major difference between their computations and ours can be seen in the effect of viscocity. Above 300 km their zonal velocities are constant in altitude, at least for the L.T. presented in their paper; however, the meridional wind component increases from 175 m/sec at 300 km to 230 m/sec at 500 km. It only becomes altitude independent above 600 km, as seen in their Figure 7. Our velocities are constant within 10% above 300 km. Though we have allowed for a diurnal and semi-diurnal variation in the kinematic viscocity, our mean viscocity values are within 50% of Kohl and King's. Figure 17 illustrates the effects of variations of the viscocity coefficient; it shows that no large differences of the velocity height profile results from a variation of the viscocity coefficient of 50%. Therefore, we cannot ascribe the different behavior of the meridional velocity altitude profile to the difference of the values of the kinematic viscocity used in the two calculations. Another difference between Kohl and King (1967) and our calculations is to be found in the time of the maximum meridional winds in the southward direction. At a latitude of 51° N (Lindau) they found a time of maximum of 3 hours L.T. and upon comparison with ionospheric data (see their Figure 11) had to advance the phase artificially by two hours in order to obtain agreement with observations. Our results show the time of maximum between midnight and 1 hour L.T., making it thus unnecessary to introduce an artificial phase shift in order to obtain agreement with observations. However, the magnitude of our neutral winds during daytime is smaller than Kohl and King have deduced. This is partly due to the differing assumptions regarding solar activity and the neglect of the average meridional wind component by Kohl and King. Kohl, King and Eccles (1968) have solved the coupled ion continuity equations and neutral wind equations and have obtained results similar to Kohl and King (1967).

The work of Bailey et al. (1969), Cho and Yeh (1970), Bramely and Rüster (1971) consists of the solution of the coupled linear neutral wind equations and the equations of motion and continuity of the ions. These calculations were performed for a given latitude and longitude, i.e., for a specific value of the magnetic dip angle. The main interest of these calculations is the study of the effects of the neutral wind system upon the ionospheric F- layer. However, the work of Bailey et al. shows that the phase of the neutral winds are little affected by the interaction of the ion and neutral wind velocity, though the magnitudes of the neutral winds may be changed. At heights where ion drag is dominant we may expect our results to differ from the above mentioned authors, because the local magnetic dip angle is not identical with our aligned dipole dip angle. This influences mainly the meridional winds. An additional slight difference is introduced by our ion drag profiles that are based on the Penn State Ionospheric Model, which does not include the effects of the neutral winds upon the ion distribution.

The results of Bailey et al. are for low levels of solar activity while Cho and Yeh present calculations for a range of solar activities. The calculations of Kohl et al. (1968) are also for low levels of solar activity. Our results can therefore be compared more directly with Cho and Yeh's work for high levels of solar activity. Figure 18 illustrates the comparison of some of the results of the above mentioned authors with our results. Though the amplitudes of the winds differ in the various computations due to the different models of ion drag and levels of solar activity, some general conclusions may be drawn:

1. The time of the maximum of the southward meridional wind is earlier in our calculations than in most others.
2. The time at which the meridional wind changes from southward to a northward direction in the northern hemisphere is less well defined in our calculation than in others. In our calculation it lingers longer near a zero level due to the presence of an average and semi-diurnal component in addition to the diurnal component. Thus, our calculations show a near zero level of meridional wind in the late morning hours.

As will be shown later, observations of meridional winds seem to support our results as far as the two above mentioned characteristics are concerned.

COMPARISON WITH OBSERVATION

The direct observation of neutral winds above a height of 200 km is difficult. Kent (1970), who has reviewed the various methods of observation, concludes that in this height region the only method available is satellite drag analysis. But drag analysis has up to now only yielded information on the average diurnal zonal wind velocity at low and mid-latitudes with no latitudinal resolution (King-Hele, 1970). Cloud releases are limited to a few occasions, and the possibility that they represent a sporadic situation rather than the steady state motion must always be considered. Neutral air motions may also be deduced from observations of the plasma motions. The most promising method of observation is the Thomson scatter technique (Evans, 1971 and 1972).

The incoherent radar back scatter technique observes the ion drift velocities which depend on three parameters: (1) The electric fields which cause ion drifts perpendicular to the electric and magnetic fields. (2) Ion diffusion velocities which are caused by pressure gradients of the various ion species and the diffusion effects of the ion-neutral system. (3) The neutral wind component in the direction of the geomagnetic field. Observation of the ion motions in the zonal direction allows one to deduce the meridional electric fields which contribute to these motions. These electric fields may be incorporated into the equations of motion of the neutral atmosphere as they modify the ion drag term (1.42). The neutral zonal motion itself cannot be deduced from the ion motion so that the method does not make it possible to compare the theoretically deduced zonal winds with observations.

The situation with regard to the meridional wind is better. If all three components of the ion drift are observed, or at least the vertical and the azimuthal drift, then both electric fields and meridional neutral motion may be uniquely determined. This determination assumes that the electric fields are perpendicular to the geomagnetic field and that the component of the ion velocity due to diffusion effects is correctly included. While the first assumption is very plausible, the second has some uncertainty. The ion motion in three perpendicular directions has only recently been determined (Woodman) and results are limited to only a few locations. If only the vertical ion drift velocity is known, then there remains an uncertainty in the neutral wind determination as both the electric fields and the neutral winds contribute to the ion drift velocity. Mostly it is only the vertical ion drift that is observed. It is therefore necessary to estimate the electric fields from other considerations or observations in order to determine the meridional winds. This is at present only possible with a limited accuracy. The effects of the ion diffusion velocity must be eliminated by a theoretical calculation before the neutral meridional winds can be determined. It has been found that the observed ion drift velocity and the calculated ion diffusion velocity are of the same order of magnitude over a considerable part of the diurnal cycle (Evans, 1971). As the neutral meridional winds are obtained from the difference of these two velocities, the accuracy of the neutral wind determination is limited. For this reason not too much significance should be ascribed to the finer details of the neutral velocity variation as deduced from this scheme. This is especially true for the exact time of the reversal of direction of the neutral winds.

We may summarize the difficulties of estimating the neutral meridional winds from incoherent scatter observations as follows: (1) The effects of neutral winds, electric fields and plasma diffusion are difficult to separate. (2) Deductions regarding the zonal wind field are impossible, or at least very uncertain. (3) If the geomagnetic declination is not zero, then the effects of zonal and meridional winds on the vertical ion velocity are intermixed. (4) The latitudinal dependence of the meridional velocities cannot be fully ascertained as only relatively few Thomson scatter stations exist.

Estimates of neutral meridional winds based on observations of the ion velocities have been made by Vasseur (1969a and 1969b), by Amayenc and Vasseur (1972a and 1972b), Evans (1971) and Harper (1971). We shall compare some of these observations with our theoretical results. For a correct interpretation of the comparison we emphasize the following points:

1. Our results refer to the global wind field; while observations using the incoherent scatter technique, even when made over prolonged periods of time, refer to the local wind field. The latter may deviate appreciably from the global winds due to effects of geomagnetic declination, a difference between geomagnetic and geographic latitude and other purely longitudinal (not local time) effects.
2. Our time resolution is six hours or less; incoherent scatter based observations have a finer time resolution.

We shall first compare our results with Vasseur's and Amayenc and Vasseur's observations. There are only minor differences between the meridional winds presented in the papers of the above authors, so that it is sufficient to take one of the results as representative.

For equinox conditions we have compared our results shown in Figure 19 with Amayenc and Vasseurs (1972a) as shown in their Figure 9. It is seen that the time of the maximum equatorward velocity is about 24 hrs for both the observationally deduced winds and our results. On the other hand, our peak velocity is almost 200 m/sec while the observationally deduced velocities are about 100 m/sec. Amayenc and Vasseur also calculate theoretical meridional winds—using their observed ion densities and the Jacchia model either without or with electric fields according to Maeda (1963). From their Figure 9 it is seen that the time of the maximum velocity we have deduced fits the observations better than their theoretically computed meridional flow. The rather considerable difference in the peak velocities may be due to a lower ion density we have used.

A comparison of our results and Amayenc and Vasseur's results for solstice conditions is shown in Figure 20. It is seen that the discrepancy in the maximum velocities between their observationally deduced results and our theoretical results has decreased as compared with equinox conditions. The times of maximum flow nearly coincide. Again, our theoretical results seem to fit the observations better than their theoretically deduced winds that are also shown in Figure 20. We cannot find any support for Amayenc and Vasseur's (1972a and 1972b) suggestion that either the pressure gradients of the Jacchia model have to be advanced by 4 hours or that electric fields must be present at equinox and summer conditions but not during winter. While, for the reasons already stated we cannot expect that our theoretical results will reproduce accurately the winds present at a particular geographical location, we nevertheless find, at least for this case, no need to assume essentially different forces from those we have included in our calculation.

Evans (1971) has determined the neutral meridional flow at Millstone Hill (42.6°N) for spring equinox conditions of the years 1969 and 1970. Figure 21 shows his results and our theoretical computations. Our results show a larger equatorward average component than Evans' observations, but the general shape and the time of the extremes are close, if the higher Fourier components are filtered out from Evans observations. These higher Fourier components are probably due to variations of ion densities which we have not included or smoothed out.

Harper (1971) has deduced neutral meridional winds at Aricebo (18° N). Figure 22 compares his results at equinox with our computation. As the difference between the geomagnetic and geographic latitude of Aricebo is 12° we have compared with our results for a mean geographic latitude averaged between geomagnetic and geographic latitudes of Aricebo. Again, when only the first two Fourier coefficients of Harper's observations are considered, the main difference between our result and his observation is the larger equatorward diurnal mean velocity which we have obtained. There is also a difference in the times of the maximum flow, which is between 23 and 24 hours according to the observations and at 1 hour L. T. according to our theoretical computations.

THE DIURNAL AVERAGE MERIDIONAL WIND

Our calculations result in an equatorward mean meridional wind at equinox conditions in both hemispheres. This wind has a velocity of 50 m/sec at a colatitude of about 50° as seen from Figure 5. This behavior is generally confirmed by observationally deduced mean meridional velocities. In the equatorial regions at +10° latitude a sharp increase of the mean velocity is calculated. This results from the non-linear coupling and the decrease of ion drag in this region. The linear solution shows also large velocity gradients in this region. We cannot state with certainty whether physical significance should be attached to the average meridional winds near the equator for the following reasons: (1) The pressure gradients deduced from the Jacchia model may be too large in the equatorial zone. They become zero at the equator but approach the zero value linearly. In reality the approach to zero may be of higher order; i. e., the equatorial horizontal pressure profile is flatter than indicated by Jacchia's model. (2) The ion drag is uncertain in this region due to the deviation of the geomagnetic field from our approximation. (3) Our results may not fulfill the differential equation with sufficient accuracy due to the strong velocity gradients relative to the mesh size.

At solstice conditions our calculations result in an even higher mean meridional wind than at equinox as is seen from Figure 6. The maximum meridional velocity during the diurnal cycle becomes as high as 350 m/sec (Figure 15). No such winds are observed although no definite conclusion should be derived from this as the high winds occur in a narrow latitude belt, and only very few observational results exist for the equatorial regions. Only the incoherent radar back scatter stations at Jicamara which has a geographical latitude of 11.9° S and a geomagnetic latitude of 2° N could possibly observe these winds. The station at Aricebo, while near the geographic equator (18° N), has a high geomagnetic latitude of 30° N. The strong mean winds which are derived from our computation result from the finite mean pressure gradients at the equator under solstice conditions that are a property of the Jacchia model (Figure 6). From the OGO-6 results (Hedin et al. 1973) it can be deduced that at a latitude belt near the equator the mean diurnal pressure gradients at solstice almost vanish. According to the analysis of the OGO-6 data this zero pressure gradient zone is not at the equator but at a latitude of about 20° N at summer solstice. For this reason the mean meridional winds at the equator are not reduced when the OGO-6 model is used instead of the Jacchia model. It may well be that at solstice a vanishing mean pressure gradient exists at the equator and not at a latitude of 20°, or alternatively the latitudinal region of zero diurnal mean meridional pressure gradients is of larger extent. If we assume this to be the case and recalculate the meridional wind velocity with the revised pressure gradients, it is found that the mean meridional wind is drastically reduced. A test calculation was performed by us with pressure gradients derived from a modified Jacchia model that was flatter at the equator and had at solstice zero mean pressure gradients of the equator. The modification kept the polar and equitorial temperatures of the Jacchia model unchanged. The mean meridional winds were reduced by about 100 m/sec as compared to the original computation. The results are presented in Figure 23. For the above reason we would like to reserve our judgement on the problem whether the diurnal mean meridional winds that are deduced from the Jacchia model are in accordance with the physical condition of the real atmosphere or whether much lower mean meridional winds exist. With the development of reliable atmospheric density models of high latitudinal resolution the problem will probably be decided.

EFFECT OF THE HORIZONTAL WIND ON THE VERTICAL VELOCITIES

If the horizontal velocities have a non-vanishing divergence of flow, then they induce a vertical velocity that is additional to the barometric velocity of the thermosphere. Rishbeth et al. (1969) have called this the vertical divergence velocity, and we shall follow their nomenclature. The horizontal divergence of the velocity is an important quantity in the dynamics of the thermosphere as it influences the energy balance through the term p div v that appears in the energy equation. This term may contribute to the observed deviation of the time of the maximum density from the values expected from simple dynamic considerations. It also may cause deviations from diffusive equilibrium of a minor constituent due to the inclusion of the horizontal divergence of flux in the continuity equation of each atmospheric constituent. The computation of the divergence velocity from $\mathrm{div}_h\ \rho v$ due to horizontal motions encounters some difficulties. The vertical divergence velocity $v_z^{(d)}$ is given by

$$V_z^{(d)}(z) = \frac{\rho(z_0)}{\rho(z)} V_z^{(d)}(z_0) + \frac{1}{\rho(z)} \int_z^{z_0} \mathrm{div}_h\,(\rho v)\,dz \tag{2.4}$$

If z_0 denotes the upper boundary at a height assumed to be near 500 km, then $\rho\ (z_0)V_z^{(d)}(z_0)$ is a flux at the upper boundary. The first term of (2.4) decreases exponentially with decreasing altitudes; therefore, the determination of divergence velocity at lower altitudes becomes almost independent of the assumptions regarding the flux at the upper boundary. It is also seen from equation (2.4) that the resulting velocity $V_z^{(d)}$ is heavily biased by the velocity divergence at lower altitudes. As no reliable data exist on the density variations in the lower thermosphere, the determination of $\mathrm{div}_h\,\rho\,v$ in the lower thermosphere where it contributes most to the energy balance becomes very uncertain. Rishbeth et al. (1969) have calculated the vertical divergence velocity from their solution of the equations of horizontal motion given by Bailey et al. (1969) at a latitude of 45° N. The accuracy of the horizontal wind field needed to compute the horizontal divergence is high, as the divergence operator requires the knowledge of velocity differences and not only of the velocities themselves. According to our results the changes of the velocity caused by the non-linear terms at the latitude of 45° are about 10%. This is more than the velocity difference between points that differ by 2° latitude which Rishbeth et al. have used in order to determine the velocity differences. Unless the influence of the non-linear terms is uniform, one would not expect much physical significance from a deduction of the divergence based on a linear calculation of the horizontal velocities. In any case near the equator a uniform influence of the non-linear terms is not to be expected.

We have performed a calculation of the horizontal velocity divergence and the vertical divergence velocity that is obtained from our horizontal velocity distribution. Figure 24 shows the mean diurnal values of the horizontal divergence at 300 km for solstice conditions. For equinox, where we assume that our results are more accurate than at solstice, we have presented in Figure 25 the values of the diurnal mean vertical divergence velocity at 130 and 300 km. In Figure 26 the circulation cells that correspond to these vertical velocities are shown. The diurnal variation of velocity divergence is of the same order of magnitude as the diurnal mean values. Our values at 300 km are significantly lower than the vertical divergence velocity deduced by Rishbeth et al. Due to the high accuracy with which the horizontal wind field is required to be known when significant results for the vertical divergence velocity are to be obtained, we would like to leave the physical significance of our vertical divergence velocities and the circulation cells that are deduced from them an open question.

The same applies to calculations of the vertical divergence velocity by other authors (Stubbe, 1972), especially as these have neglected many terms of the equations of motion which we have included. A treatment of thermospheric dynamics that is completely self-consistent and does not rely on given empirical models may avoid these difficulties and render a better approximation for the vertical divergence velocities.

DISCUSSION OF THE TERMS OF THE EQUATIONS OF MOTION

In most previous investigations the equations of motion were simplified by neglecting some of the terms appearing in them. Furthermore, sometimes a certain term was artifically enhanced in order to compensate for the dropping of another term; for instance, Volland et al. (1971) have excluded viscocity effects but included an enhanced ion drag term. The relative magnitude of the various terms of the equations of motion and their contribution to the balancing of the equation is therefore of considerable interest as it is a measure for the admissibility and accuracy of the various approximations.

Connected with this problem is also the effect that a change in coefficient of ion drag and viscous drag has on the solution of the equations. For the linearized equations we have performed test calculations where the ion drag and the viscous drag coefficients were changed by factors varying between 0.25 and 1.5. The effect of these changes is shown in Figure 27 for the ion drag. As to be expected, the change of the velocities is inversely proportional to the drag coefficient.

For the viscocity coefficient this is shown in Figure 17. For the meridional component shown in this figure the effect of a change in the viscocity coefficient is similar to the effect of a change of the ion drag coefficient. This is not true for all Fourier components of the velocity distribution. A viscous drag can also cause an increase of a velocity component by an interaction of the various Fourier modes. This difference in the behavior between ion drag and viscocity is understandable, as the ion drag multiplies the velocity where as the viscocity coefficient multiplies the second derivative of velocity. For this reason the simulation of one effect by the other should be regarded with caution.

The value of the various terms appearing in the equations of motion is illustrated for some Fourier coefficients and some local time variations in Figures 28 - 32. In line with our original equations (1.4) the terms were divided by ω and have the dimension of m/sec. It is in this sense that the "forces" that appear in the figures have to be interpreted. Generally it is seen that the non-linear terms are only of importance in the equatorial regions, there they may even be comparable to the dominating terms of the equations. The effects of horizontal viscocity, which are also dependent upon horizontal velocity gradients like the non-linear parts of the convective derivative, are likewise only of importance in the equatorial regions. For the main terms of the equations we cannot find a general rule as, for instance, the ion drag is more important than the viscocity or the driving forces are more important than the Coriolis force. For example, the mean diurnal zonal driving force is zero for all latitudes, but the mean value of the zonal viscous force is not zero. Further examples of similar behavior may be found from the figures. We conclude from this behavior that for the global description of the velocity distribution it is really not possible to simplify the equations of motion without considerable loss of accuracy. For a partial solution, i.e., one limited to a certain geographic location or to a certain height, simplifications of the equations are justified.

REFERENCES

Amayenc, P., G. Vasseur, Neutral winds deduced from incoherent scatter observations and their theoretical interpretation, Jr. Atmosph. Terr. Phys. 34, 351-364 (1972a)

Amayenc, P., G. Vasseur, Observation and interpretation of ionization drift measurements in the F region at St-Santin-Nancay, Space Research 12, 957-967, (1972b)

Bailey, G. J., R. J. Moffett, H. Rishbeth, Solution of the coupled ion and neutral air equations of the mid-latitude ionospheric layer, Jr. Atmosph. Terr. Phys. 31, 253-270, (1969)

Blum, P. W., I. Harris, Full non-linear treatment of the global thermospheric wind system, Part 1: Mathematical method and analysis of forces. Goddard Space Flight Center, No. X-621-73-35, 59 pages, (1973) Bramely, E. N., R. Rüster, The effects of electric fields and ion drag in the middle F-region, Jr. Atmosph. Terr. Phys. 33, 269-274, (1971)

Brillouin, M., Les latitudes critiques, Compt. Rend. Acad. Sci., Paris 194, 801-804, (1932)

Chiu, Y. T., The rotation rate of the upper atmosphere, a non-linear effect, Planet. Space Sci. 19, 1201-1208, (1971)

Cho, H. R., K. C. Yeh, Neutral winds and the behavior of the ionospheric F2-region, Radio Science 5, 881-894, (1970)

Evans, J. V., Observation of the F region vertical velocities at Millstone Hill, 1, Evidence for drifts due to expansion, contraction and winds, Radio Science 6, 609-626, (1971)

Evans, J. V., Ionospheric movements measured by incoherent scatter: A review, Jr. Atmosph. Terr. Phys. 34, 175-209, (1972)

Geisler, J. E., A numerical study of the wind system in the middle thermosphere, Jr. Atmosph. Terr. Phys. 29, 1469-1482, (1967)

Harper, R. M., Dynamics of the neutral atmosphere in the 200-500 km height region at low latitudes, Thesis, Rice University, Houston, Texas, (1971) Hedin, A. E., H. G. Mayr, C. A. Reber, N. W. Spencer, G. R. Carignan, Empirical model of global thermospheric temperature and composition based on data from the OGO-6 quadrupole mass spectrometer, Goddard Space Flight Center Report No. X-621-73-37. 65 pages, (1972)

Kallina, C., Periodicity and stability for linear and quasi-linear parabolic equations, Siam J. Appl. Math. 18, 601-608, (1970)

Kent, G. S., Measurements of Ionspheric movements, Rev. of Geophys. and Space Physics, 8, 229-288, (1970)

King-Hele, D. G., Average rotational speed of the upper atmosphere from changes in satellite orbits, Space Res. 10, 537-540, (1970)

Kohl, H., J. W. King, Atmospheric winds between 100 and 700 km and their effects on the ionosphere, Jr. Atmosph. Terr. Phys. 29, 1045-1062, (1967)

Kohl, H., J. W. King, D. Eccles, Some effects of neutral air winds on the ionospheric F-layer, Jr. Atmosph. Terr. Phys. 30, 1733-1744, (1968)

Maeda, H., "World-wide pattern of ionisation drifts in the ionospheric F-region", Proc. Conf. Ionospheric, London, The Institute of Physics and the Physical Society, 187-190, (1963)

Rishbeth, H., Polarization fields produced by winds in the equatorial F-region, Planet. Space Sci. 19, 357-369, (1971) Rishbeth, H., Thermospheric winds and the F region: A review, Jr. Atmosph. Terr. Phys. 34, 1-47, (1972)

Rishbeth, H., R. J. Moffett, G. H. Bailey, Continuity of air motion in the mid-latitude thermosphere, Jr. Atmosph. Terr. Phys. 31, 1035-1047, (1969)

Rüster, R., Solution of the coupled ionospheric continuity equations of motion for the ions, electrons and neutral particles, Jr. Atmosph. Terr. Phys. 33, 137-147, (1971)

Rüster, R., J. R. Dudney, The importance of the non-linear term in the equation of motion of the neutral atmosphere, Jr. Atmosph. Terr. Phys. 34, 1075-1083, (1972)

Smith, L. B., Rotation of wind direction with altitude as obtained from vapor trail observations, Jr. Geophs. Res. 77, 2927-2933, (1972)

Stubbe, P., Simultaneous solution of the time dependent coupled continuity equations, heat conduction equations and equations of motion for a system consisting of a neutral gas, an electron gas and a four component ion gas, Jr. Atmosph. Terr. Phys. 32, 865-903, (1970)

Stubbe, P., Vertical neutral gas motions and deviations from the barometric law in the lower thermosphere, Planet. Space. Sci. 20, 209-215, (1972) Vasseur, G., Vents dans la thermosphere deduits des measures par diffusion de Thomson, Ann. de Geophys. 25, 517-524, (1969a)

Vasseur, G., Dynamics of the F-region observed with Thomson scatter, I-atmospheric circulation and neutral winds, Jr. Atmosph. Terr. Phys. 31, 397-420, (1969b)

Volland, H., Mayr, H. G., A three dimensional model of thermospheric dynamics I., Jr. Atmosph. Terr. Phys. 34, 1745-1768, (1972)

Woodman, R. F., East-West ionospheric drifts at the magnetic equator, Space Research 12, 969-974, (1972)

FIGURE CAPTIONS

Figure 1. Global wind field at a height of 300 km, equinox conditions

Figure 2. Global wind field for summer solstice conditions for the Northern Hemisphere

Figure 3. Global wind field for summer solstice conditions for the Southern Hemisphere

Figure 4. Average zonal velocity, equinox conditions as a function of latitude for heights of 200, 300 and 400 km

Figure 5. Comparison of linear and non-linear amplitudes of the mean, diurnal and semi-diurnal modes of the meridional winds as a function of latitude for the height of 300 km at equinox. 0 denotes mean, 1 denotes diurnal, 2 denotes semi-diurnal. Non-linear solutions are dashed, linear solutions are shown solid

Figure 6. Comparison of linear and non-linear solutions for the average meridional velocity for solstice conditions at the height of 300 km

Figure 7. The latitudinal dependence of the time of maximum of the southward meridional wind for solstice and equinox conditions, dashed curve is the linear solution for equinox, dotted curve is the non-linear solution for equinox

Figure 8. The local time dependence of the meridional winds for equinox conditions, height 300 km, for latitudes of 10°, 30°, 50°

Figure 9. Same as Figure 8 for solstice conditions for latitudes of -10°, 0°, 10°, 30°, 50°

Figure 10. Height dependence of the amplitude of zonal wind components for solstice conditions at a latitude of -10°

Figure 11. Average zonal velocity for equinox conditions as a function of height for various latitudes for two levels of solar activity

Figure 12. Effect of lower boundary conditions upon the amplitudes of the average wind components for equinox conditions. Solid lines are for the case where the zonal and meridional velocities are zero at the lower boundary, the dotted curves for the case where the zonal velocity is 100 m/sec at the lower boundary

Figure 13. Linear and non-linear solutions of the meridional winds for latitudes of 10° and 30°, equinox conditions, height 300 km

Figure 14. Comparison of linear (solid) and non-linear (dashed) solutions of the time dependance of the meridional winds at solstice conditions, height of 300 km for latitudes of -30° and -50°

Figure 23. Mean meridional winds for a modified Jacchia model at solstice

Figure 24. The average horizontal velocity divergence at 300 km for solstice conditions

Figure 25. Diurnal mean vertical "divergence" velocities at 130 km and 300 km for equinox conditions

Figure 26. Diurnal mean latitudinal circulation cells at 130 km and 300 km for equinox conditions

Figure 27. Effect of variation of ion drag on the amplitude of the diurnal component of meridional velocity for the linear model. Four different values are illustrated from 1.5 of the normal value to 0.25 of normal value

Figure 28. Magnitude of the various terms in the equation of motion for the average meridional component at equinox, height of 300 km. VIS2 is the horizontal viscocity. All terms are brought to the lefthand side of the equation and divided by ω

Figure 29. Same as Figure 28, but for solstice conditions

Figure 30. Same as Figure 28, but for the average zonal component

Figure 31. Same as Figure 28, but for the total meridional velocity as a function of local time, at equinox

Figure 32. Same as Figure 31, but for solstice conditions

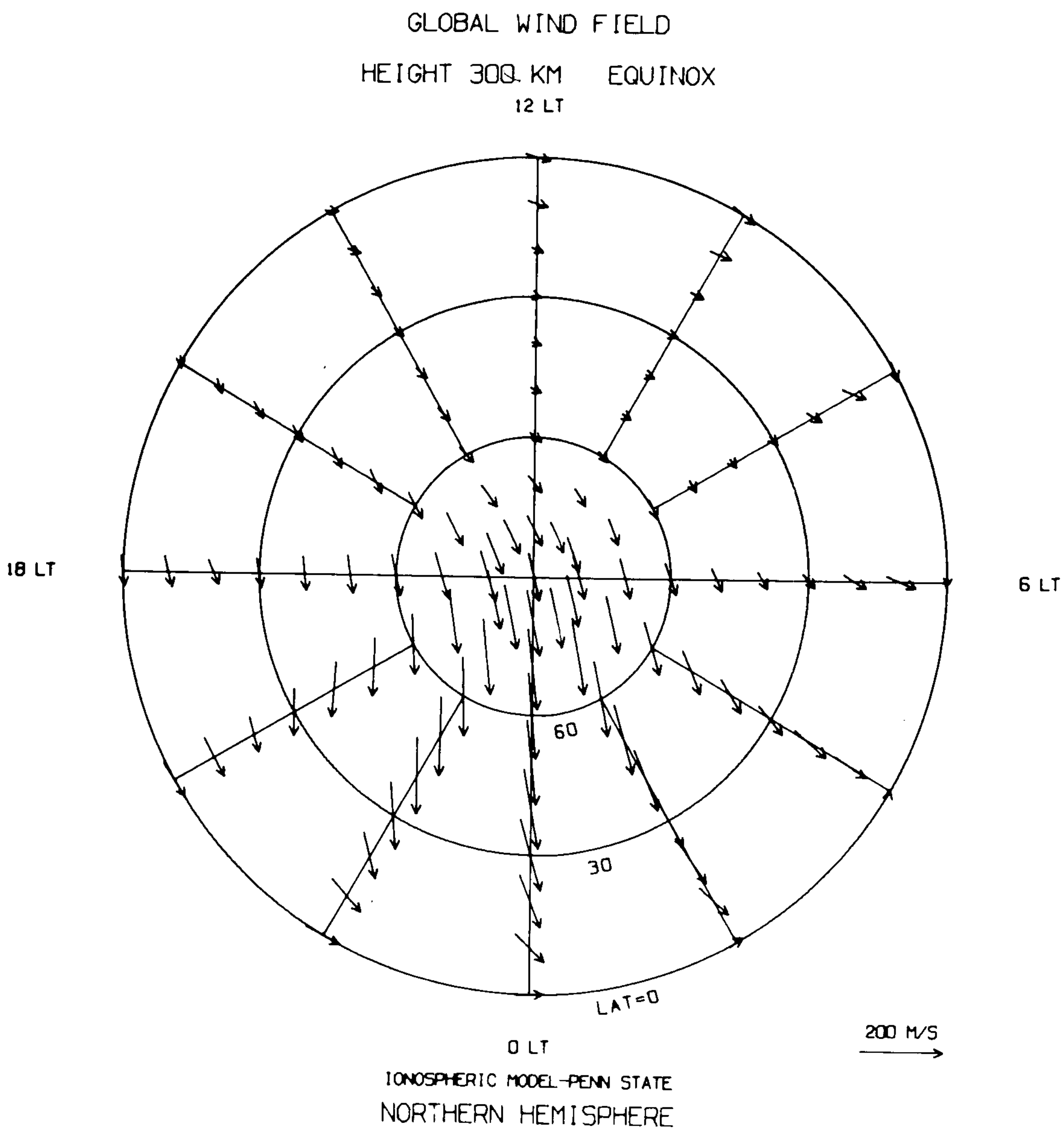
GLOBAL WIND FIELD
HEIGHT 300. KM EQUINOX
12 LT
18 LT
6 LT
60
30
LAT=0
0 LT
200 M/S
IONOSPHERIC MODEL-PENN STATE
NORTHERN HEMISPHERE

Fig. 1

GLOBAL WIND FIELD

HEIGHT 300 KM SOLSTICE

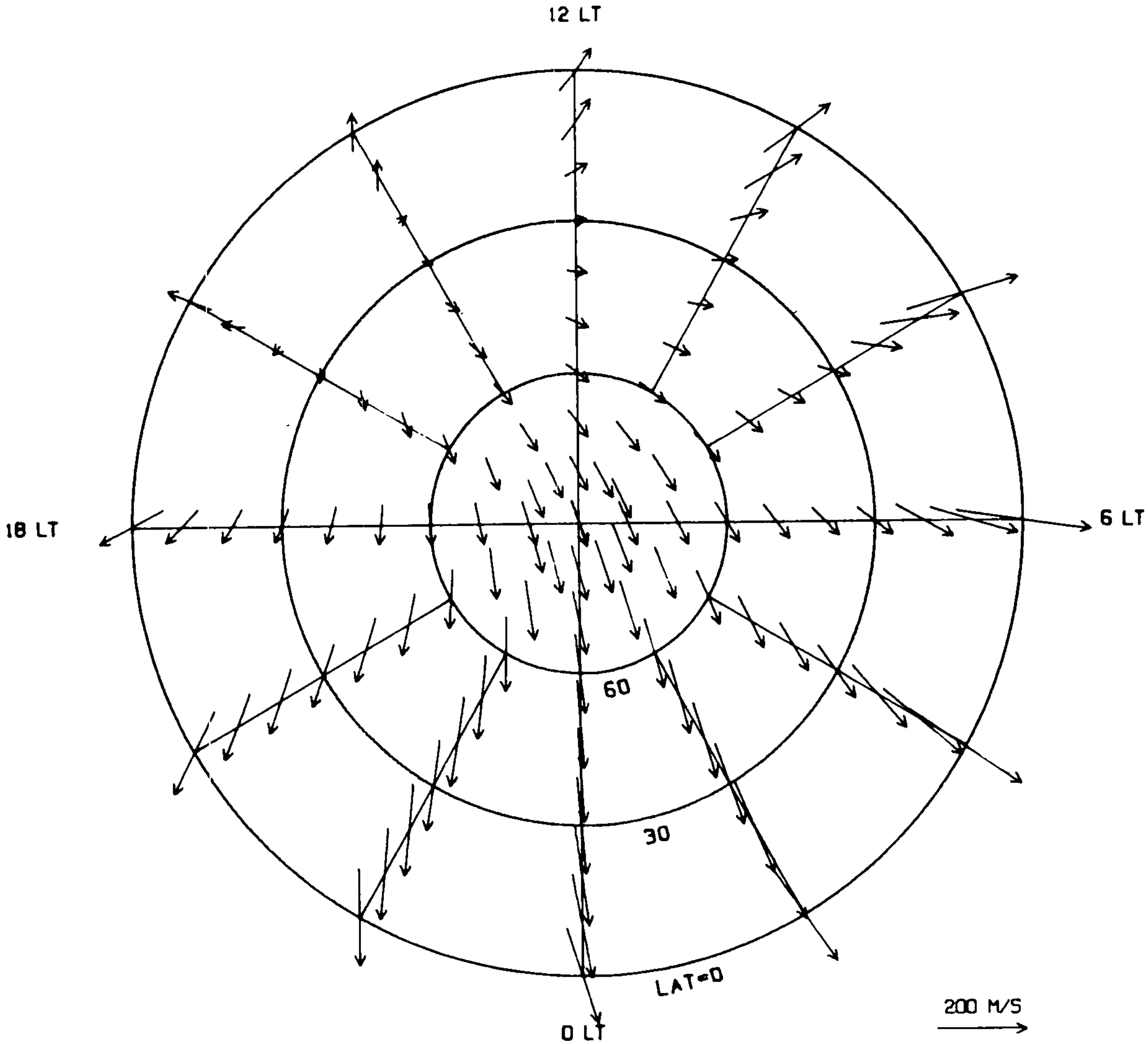

IONOSPHERIC MODEL-PENN STATE

NORTHERN HEMISPHERE

Fig. 2

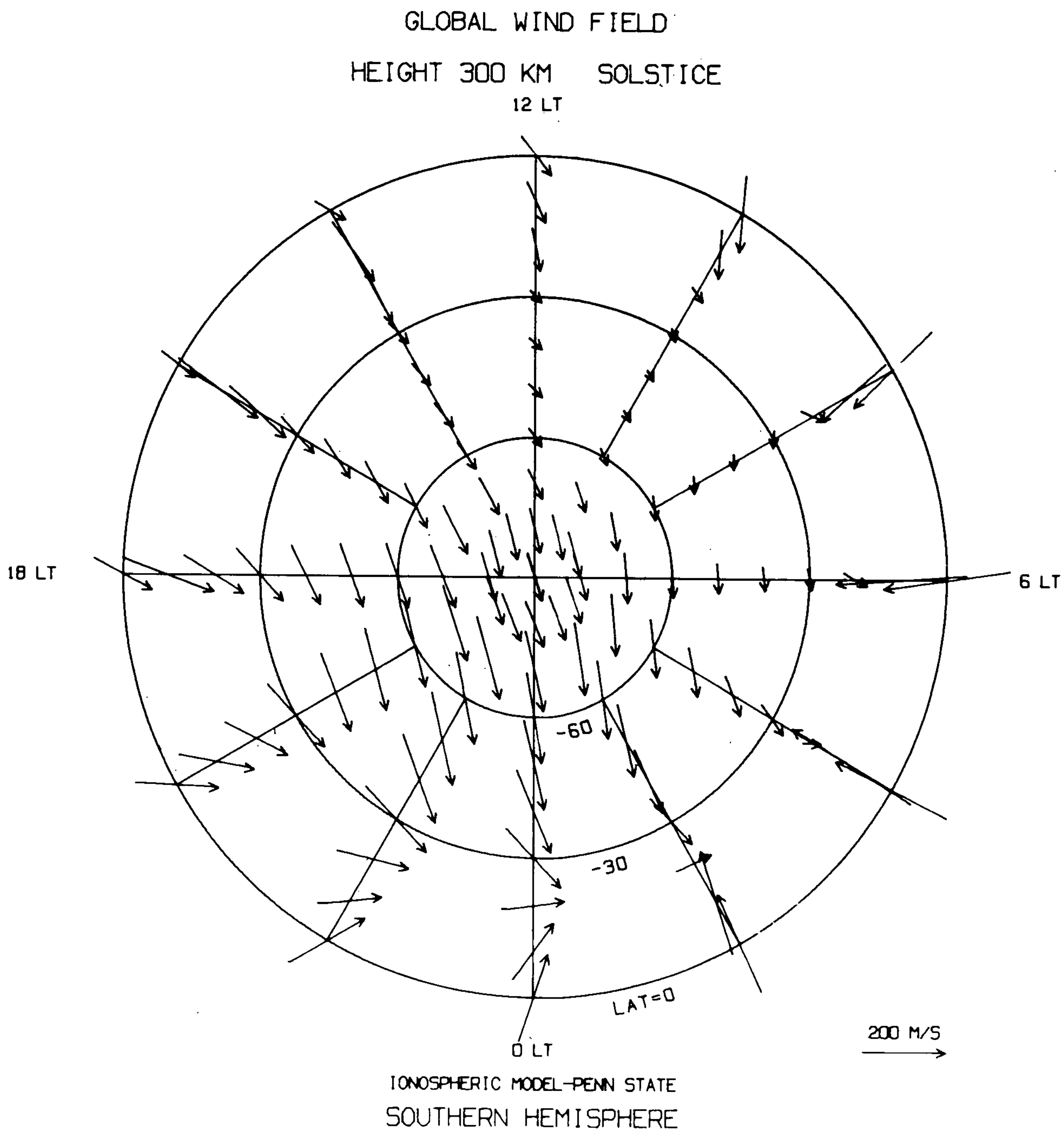
GLOBAL WIND FIELD
HEIGHT 300 KM SOLSTICE
12 LT
18 LT
6 LT
-60
-30
LAT=0
0 LT
200 M/S
IONOSPHERIC MODEL-PENN STATE
SOUTHERN HEMISPHERE

Fig. 3

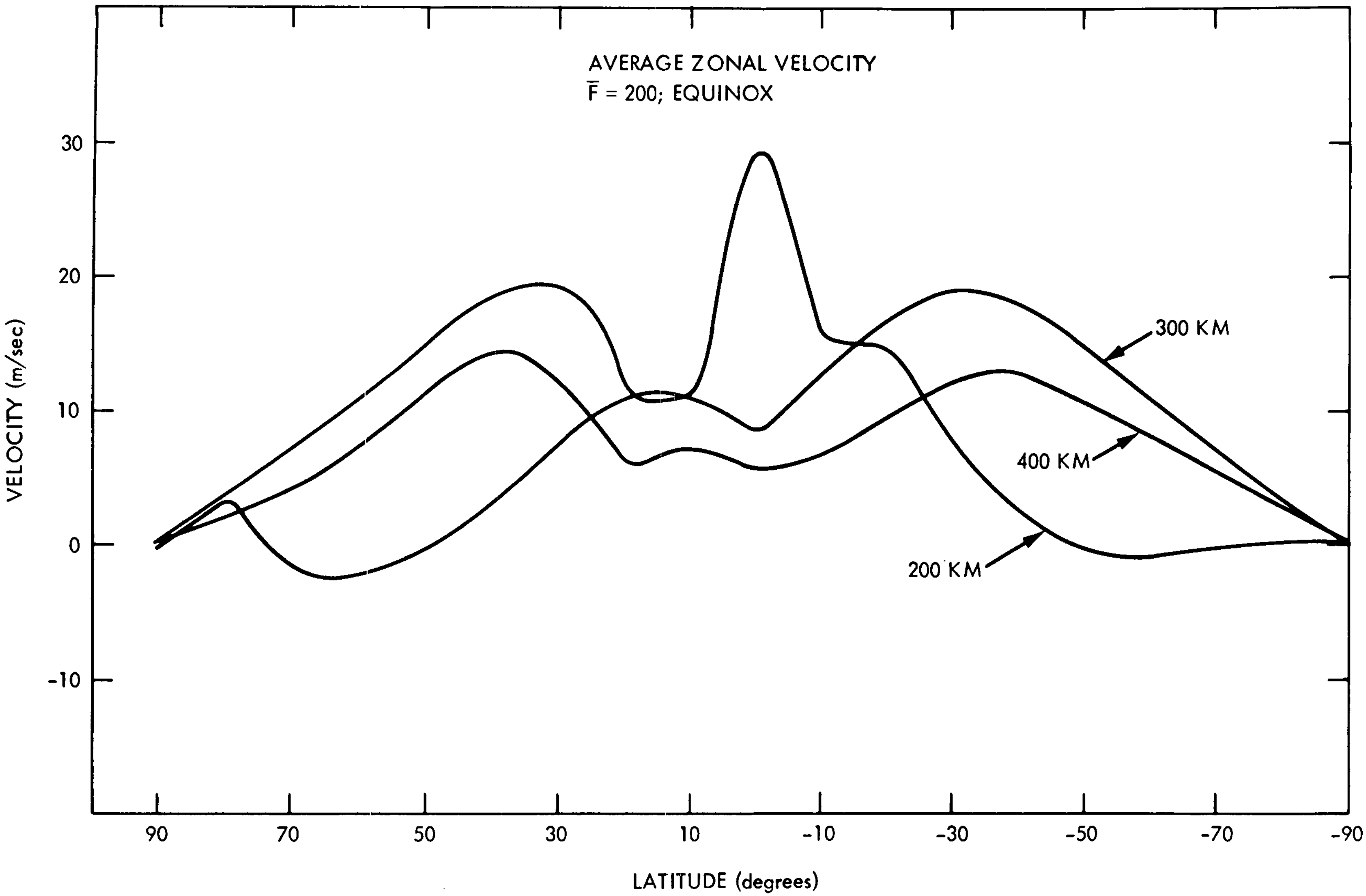
AVERAGE ZONAL VELOCITY
$\overline{F}$ = 200; EQUINOX
VELOCITY (m/sec)
30
20
10
0
-10
300 KM
400 KM
200 KM
90
70
50
30
10
-10
-30
-50
-70
-90
LATITUDE (degrees)

Fig. 4

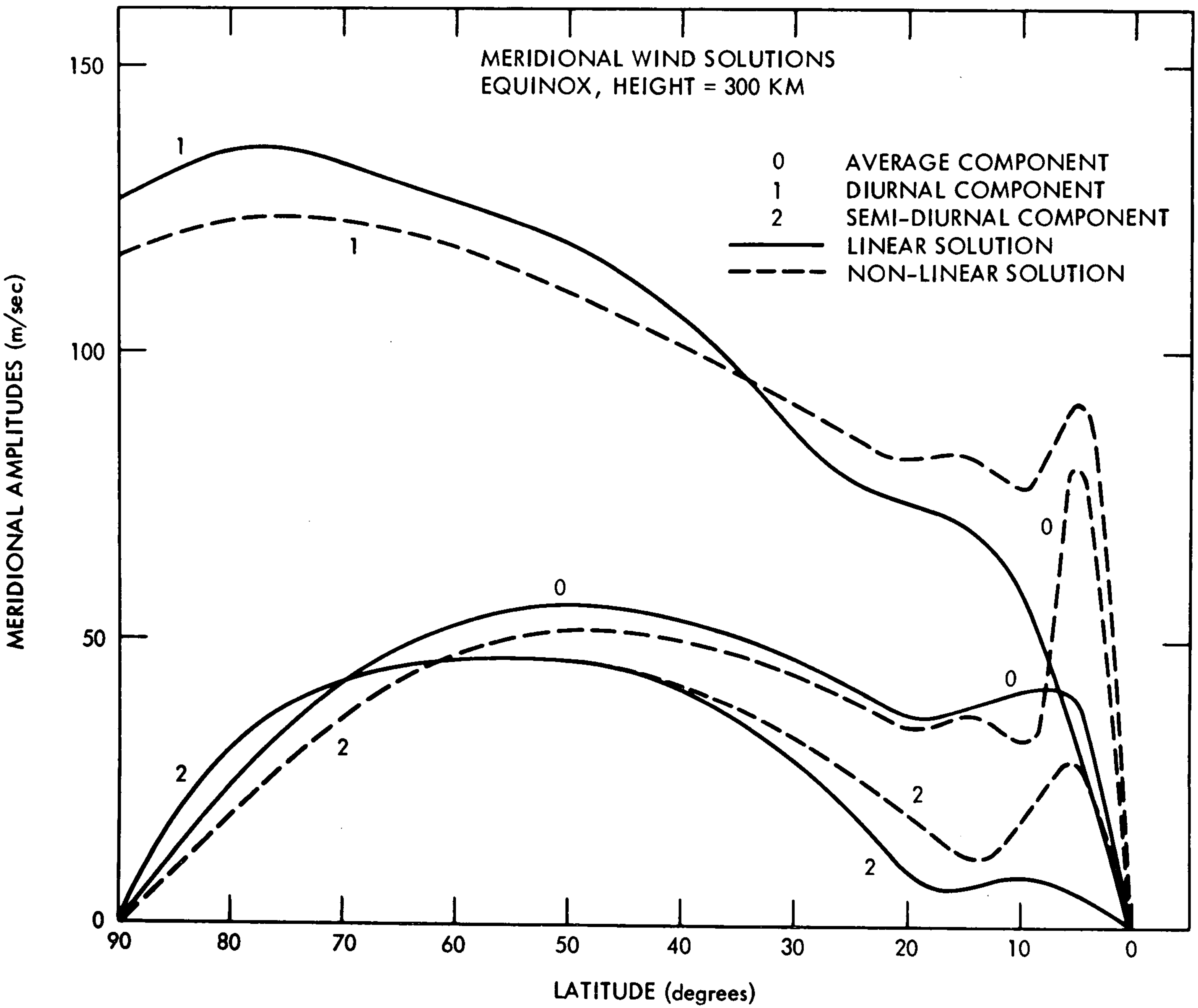

MERIDIONAL WIND SOLUTIONS
EQUINOX, HEIGHT = 300 KM
0 AVERAGE COMPONENT
1 DIURNAL COMPONENT
2 SEMI-DIURNAL COMPONENT
LINEAR SOLUTION
NON-LINEAR SOLUTION
MERIDIONAL AMPLITUDES (m/sec)
150
100
50
0
90
80
70
60
50
40
30
20
10
0
LATITUDE (degrees)

Fig. 5

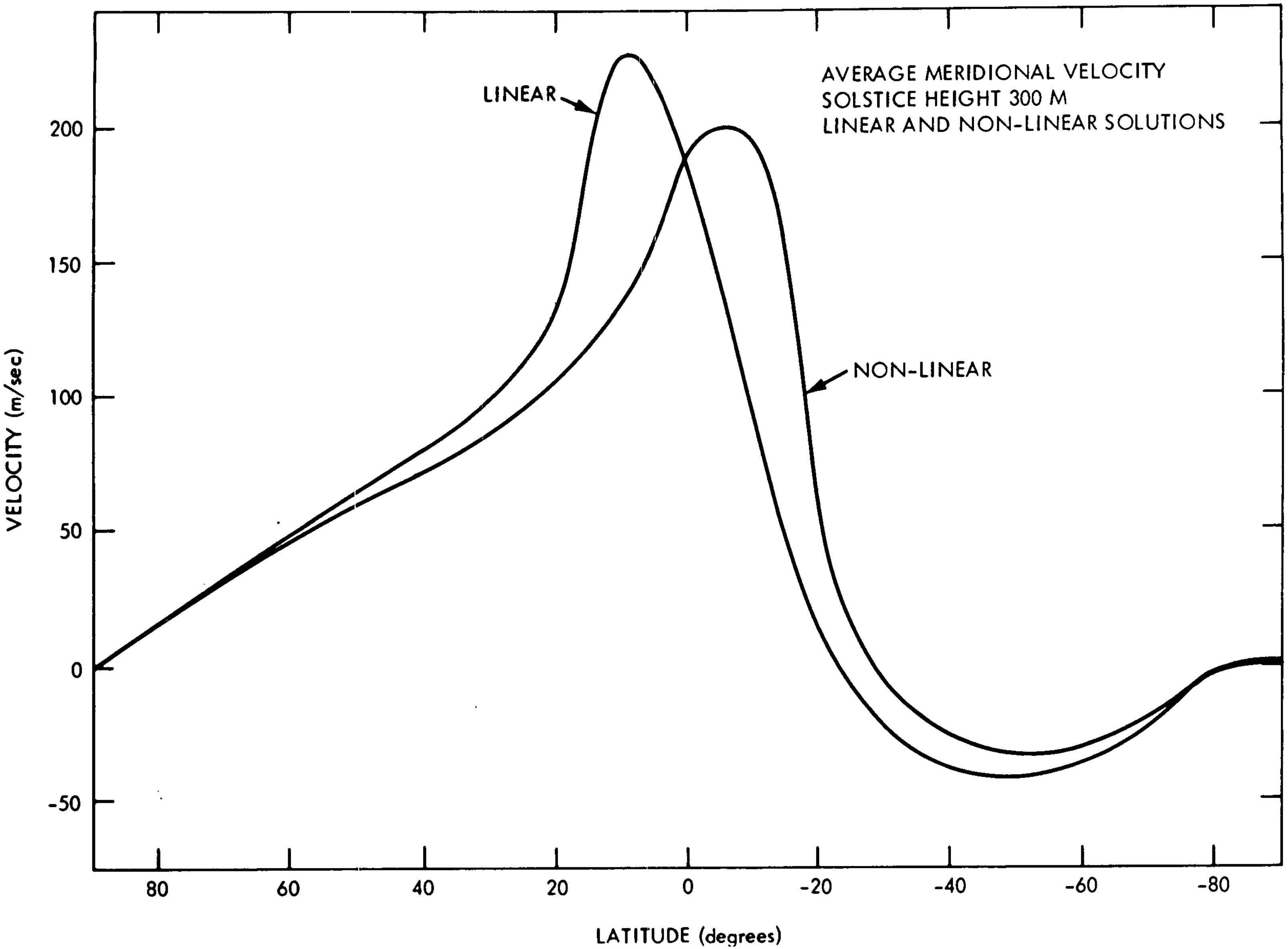
AVERAGE MERIDIONAL VELOCITY
SOLSTICE HEIGHT 300 M
LINEAR AND NON-LINEAR SOLUTIONS
LINEAR
NON-LINEAR
VELOCITY (m/sec)
200
150
100
50
0
-50
80
60
40
20
0
-20
-40
-60
-80
LATITUDE (degrees)

Fig. 6

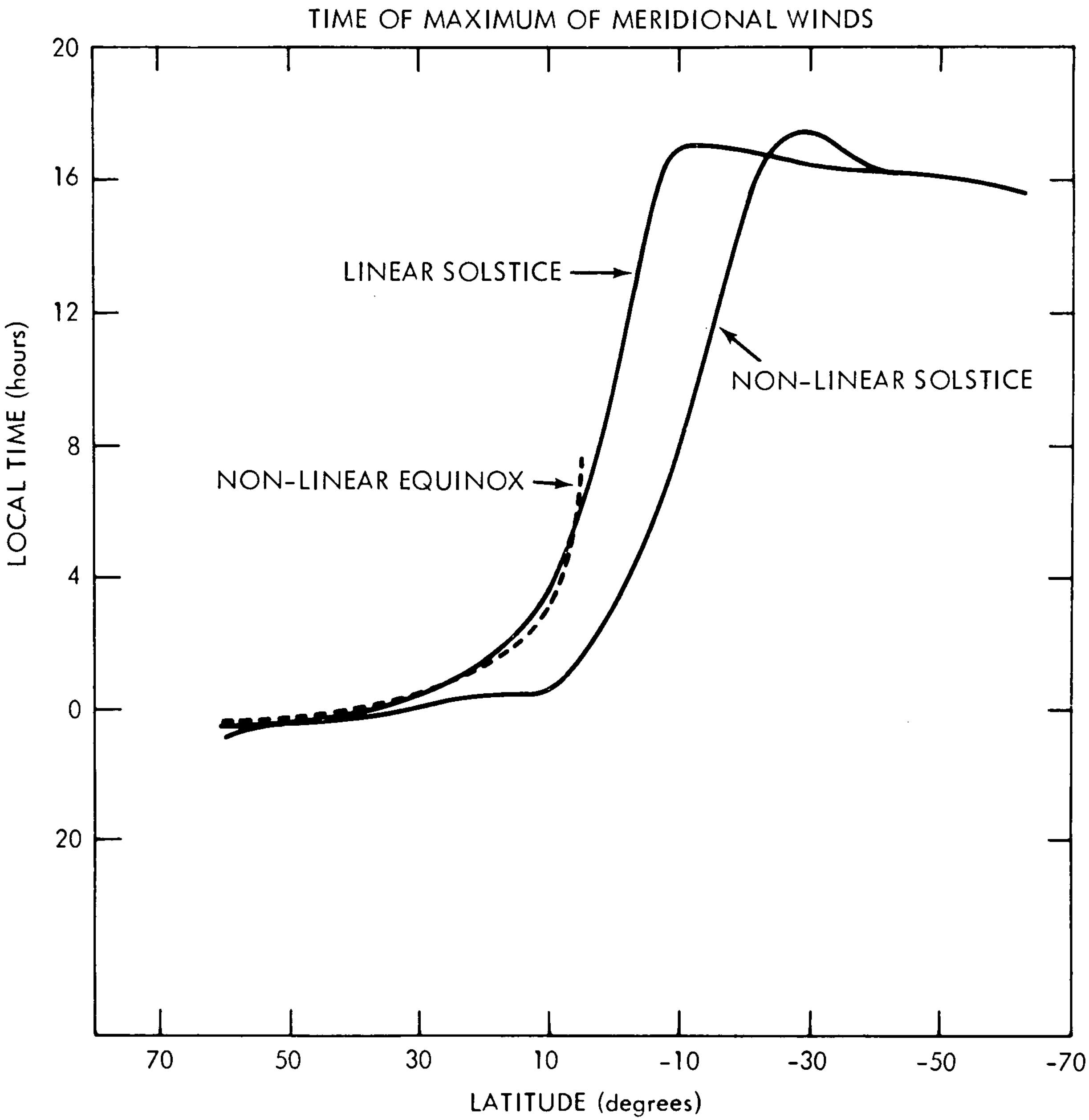
TIME OF MAXIMUM OF MERIDIONAL WINDS
LINEAR SOLSTICE
NON-LINEAR SOLSTICE
NON-LINEAR EQUINOX
LOCAL TIME (hours)
LATITUDE (degrees)
20
16
12
8
4
0
20
70
50
30
10
-10
-30
-50
-70

Fig. 7

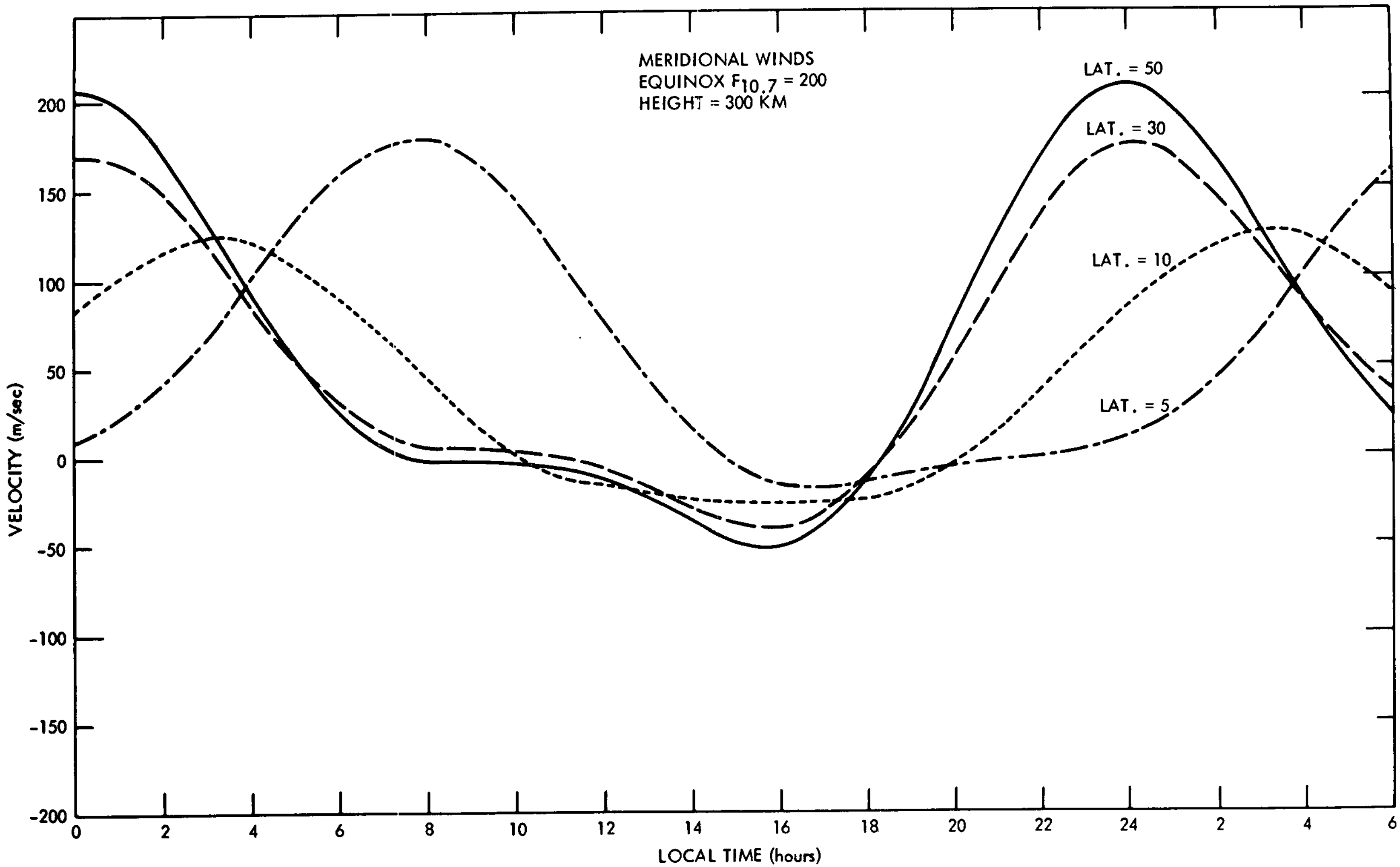
MERIDIONAL WINDS
EQUINOX $F_{10.7}$ = 200
HEIGHT = 300 KM
LAT. = 50
LAT. = 30
LAT. = 10
LAT. = 5
VELOCITY (m/sec)
200
150
100
50
0
-50
-100
-150
-200
0
2
4
6
8
10
12
14
16
18
20
22
24
2
4
6
LOCAL TIME (hours)

Fig. 8

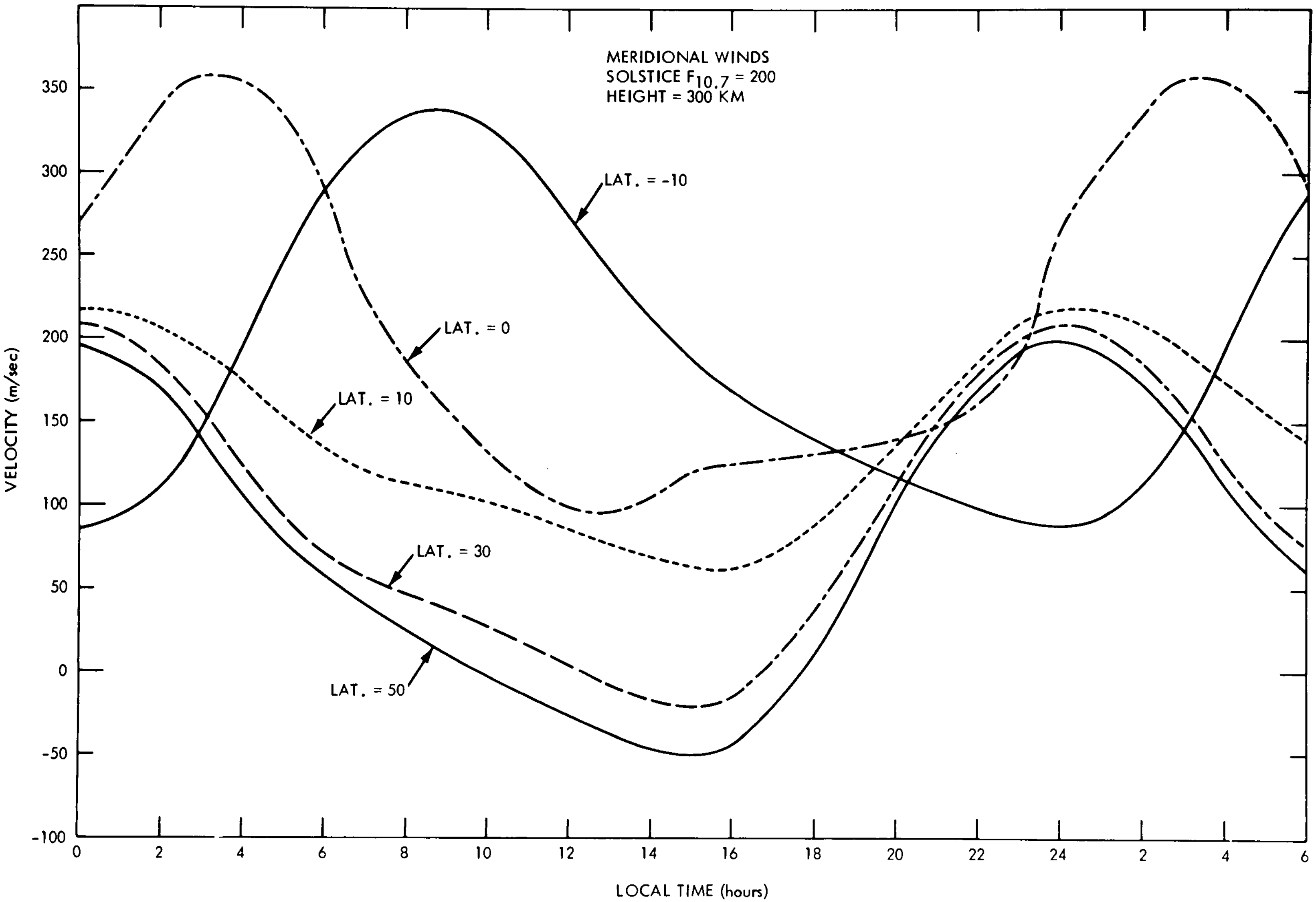
MERIDIONAL WINDS
SOLSTICE $F_{10.7}$ = 200
HEIGHT = 300 KM
LAT. = -10
LAT. = 0
LAT. = 10
LAT. = 30
LAT. = 50
VELOCITY (m/sec)
350
300
250
200
150
100
50
0
-50
-100
0 2 4 6 8 10 12 14 16 18 20 22 24 2 4 6
LOCAL TIME (hours)

Fig. 9

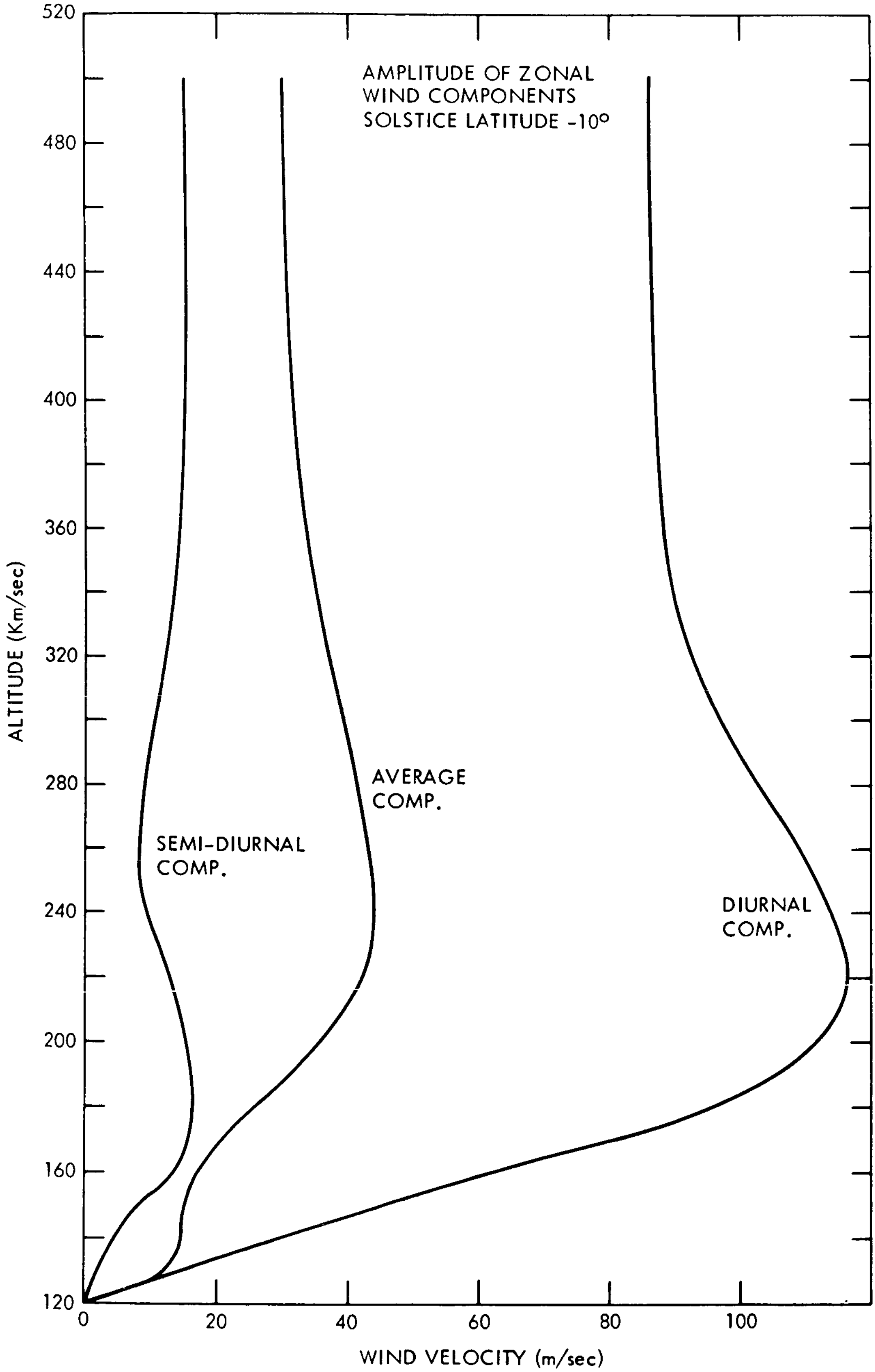
AMPLITUDE OF ZONAL
WIND COMPONENTS
SOLSTICE LATITUDE -10°
AVERAGE
COMP.
SEMI-DIURNAL
COMP.
DIURNAL
COMP.
ALTITUDE (Km/sec)
WIND VELOCITY (m/sec)
520
480
440
400
360
320
280
240
200
160
120
0
20
40
60
80
100

Fig. 10

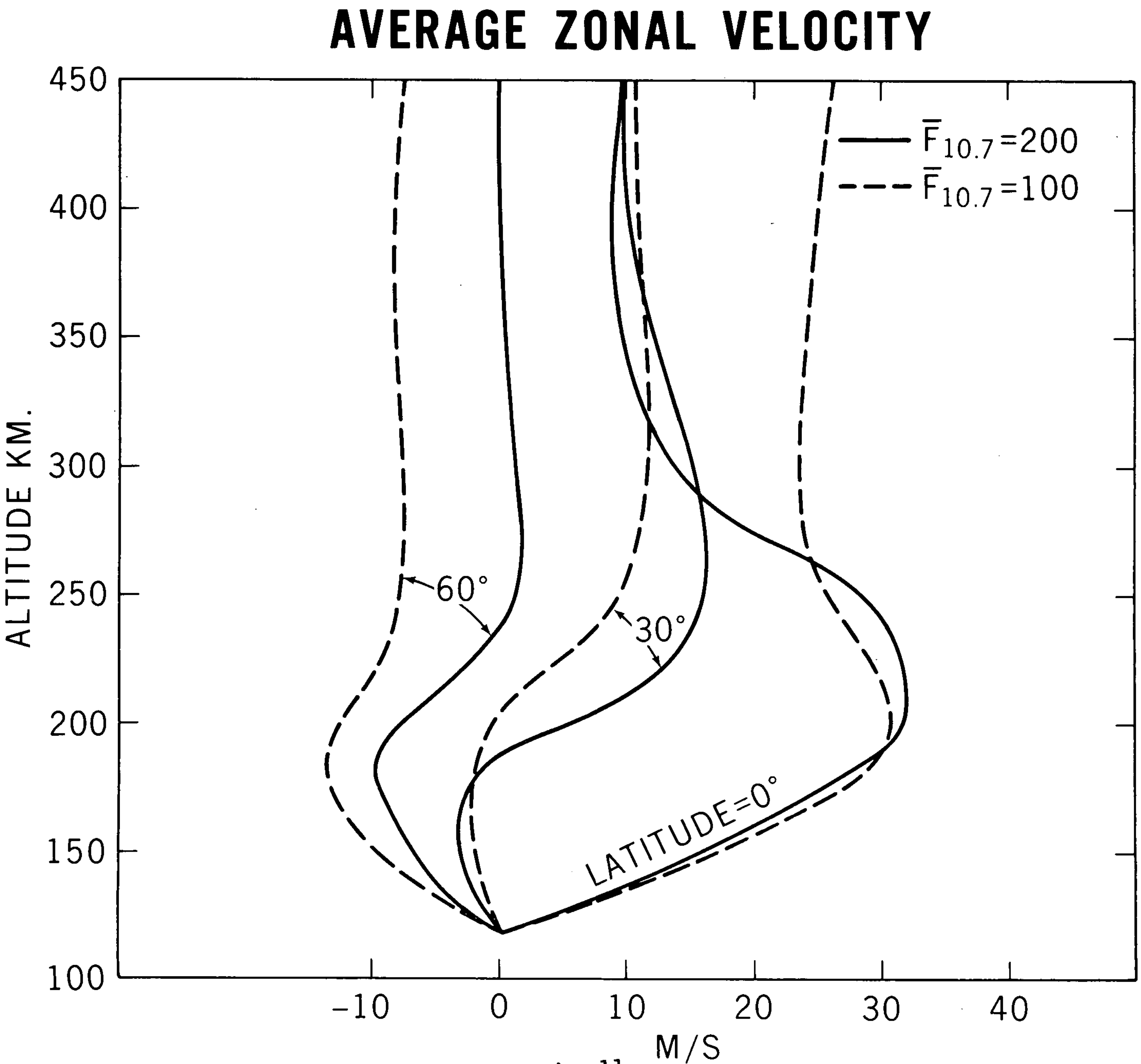
AVERAGE ZONAL VELOCITY
450
400
350
300
250
200
150
100
ALTITUDE KM.
$\bar{F}_{10.7}=200$
$\bar{F}_{10.7}=100$
60°
30°
LATITUDE=0°
-10
0
10
20
30
40
M/S

Fig. 11

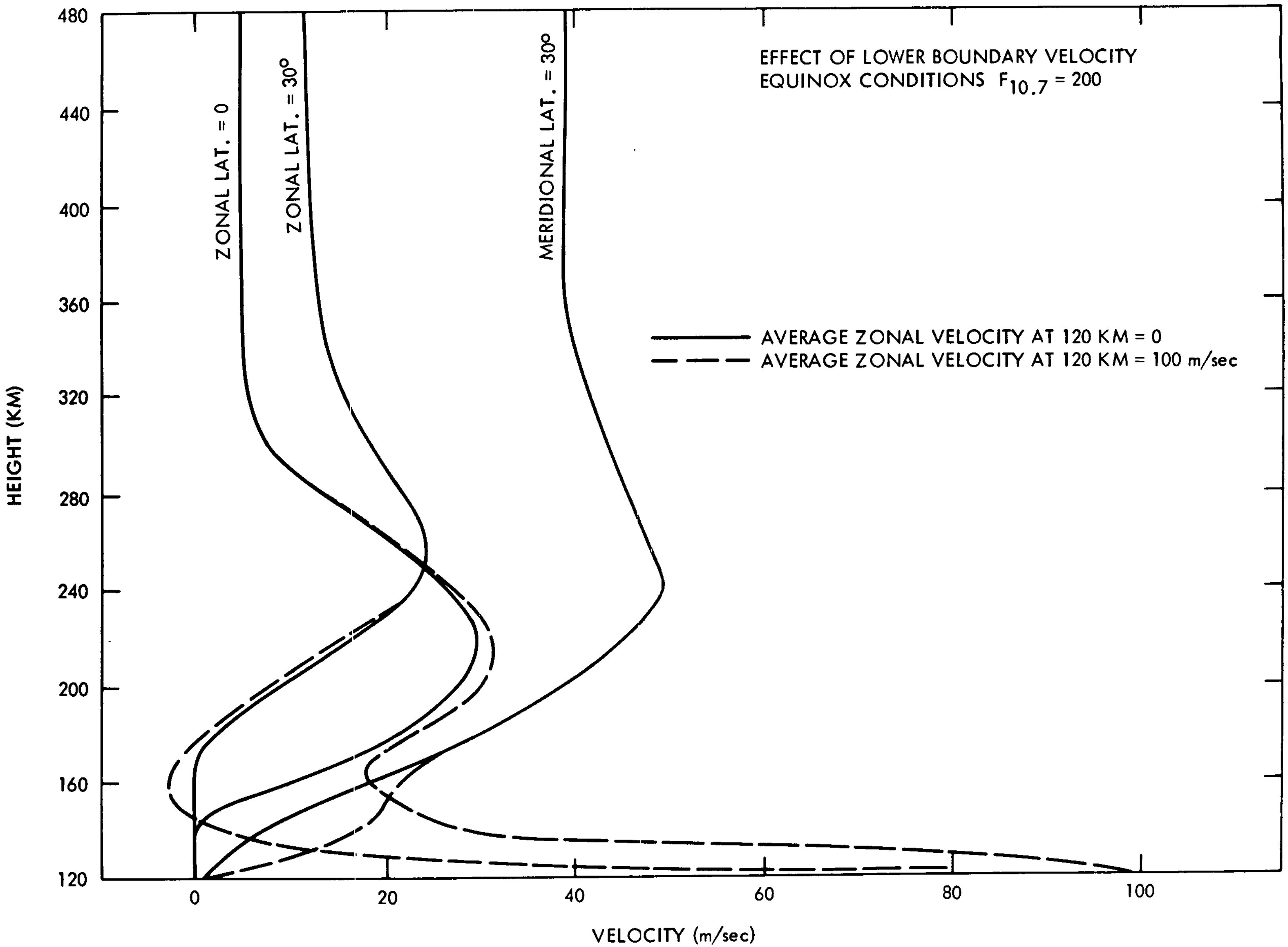
EFFECT OF LOWER BOUNDARY VELOCITY
EQUINOX CONDITIONS $F_{10.7} = 200$
ZONAL LAT. = 0
ZONAL LAT. = 30°
MERIDIONAL LAT. = 30°
AVERAGE ZONAL VELOCITY AT 120 KM = 0
AVERAGE ZONAL VELOCITY AT 120 KM = 100 m/sec
HEIGHT (KM)
480
440
400
360
320
280
240
200
160
120
0
20
40
60
80
100
VELOCITY (m/sec)

Fig. 12

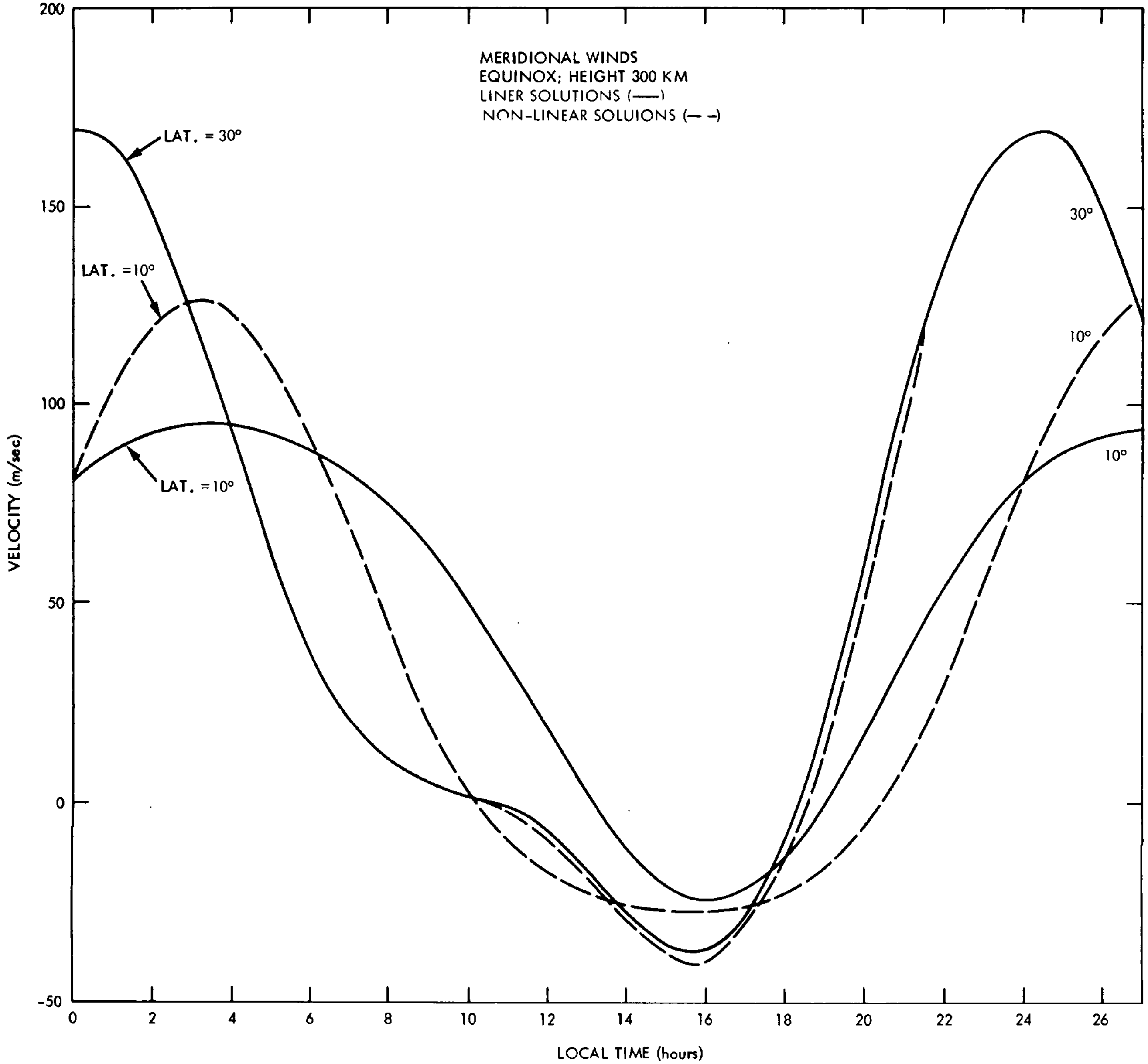
MERIDIONAL WINDS
EQUINOX; HEIGHT 300 KM
LINER SOLUTIONS (——)
NON-LINEAR SOLUIONS (— —)
LAT. = 30°
LAT. =10°
LAT. =10°
30°
10°
10°
VELOCITY (m/sec)
200
150
100
50
0
-50
0
2
4
6
8
10
12
14
16
18
20
22
24
26
LOCAL TIME (hours)

Fig. 13

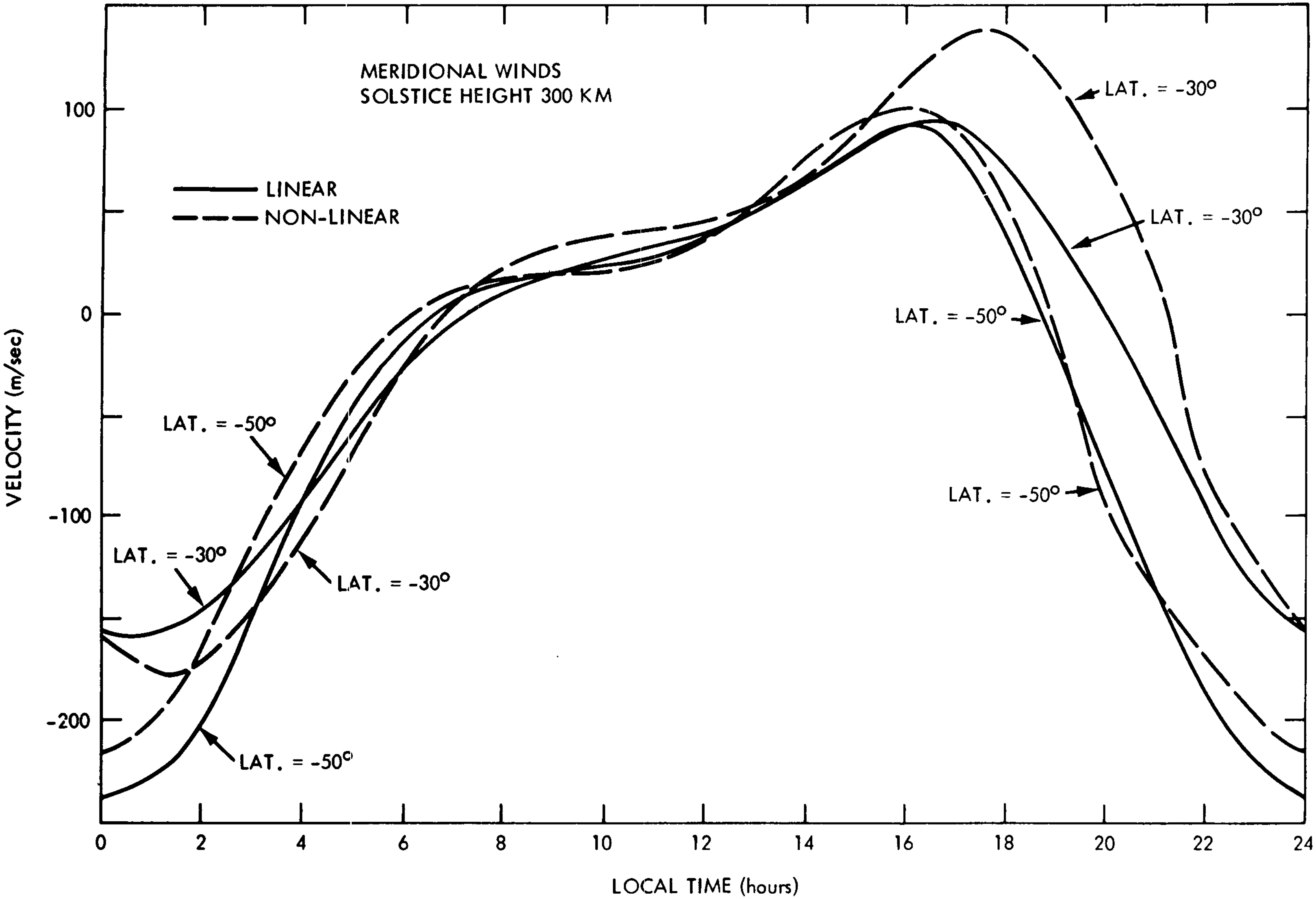
MERIDIONAL WINDS
SOLSTICE HEIGHT 300 KM
LINEAR
NON-LINEAR
LAT. = -30°
LAT. = -30°
LAT. = -50°
LAT. = -50°
LAT. = -50°
LAT. = -30°
LAT. = -30°
LAT. = -50°
VELOCITY (m/sec)
100
0
-100
-200
0
2
4
6
8
10
12
14
16
18
20
22
24
LOCAL TIME (hours)

Fig. 14

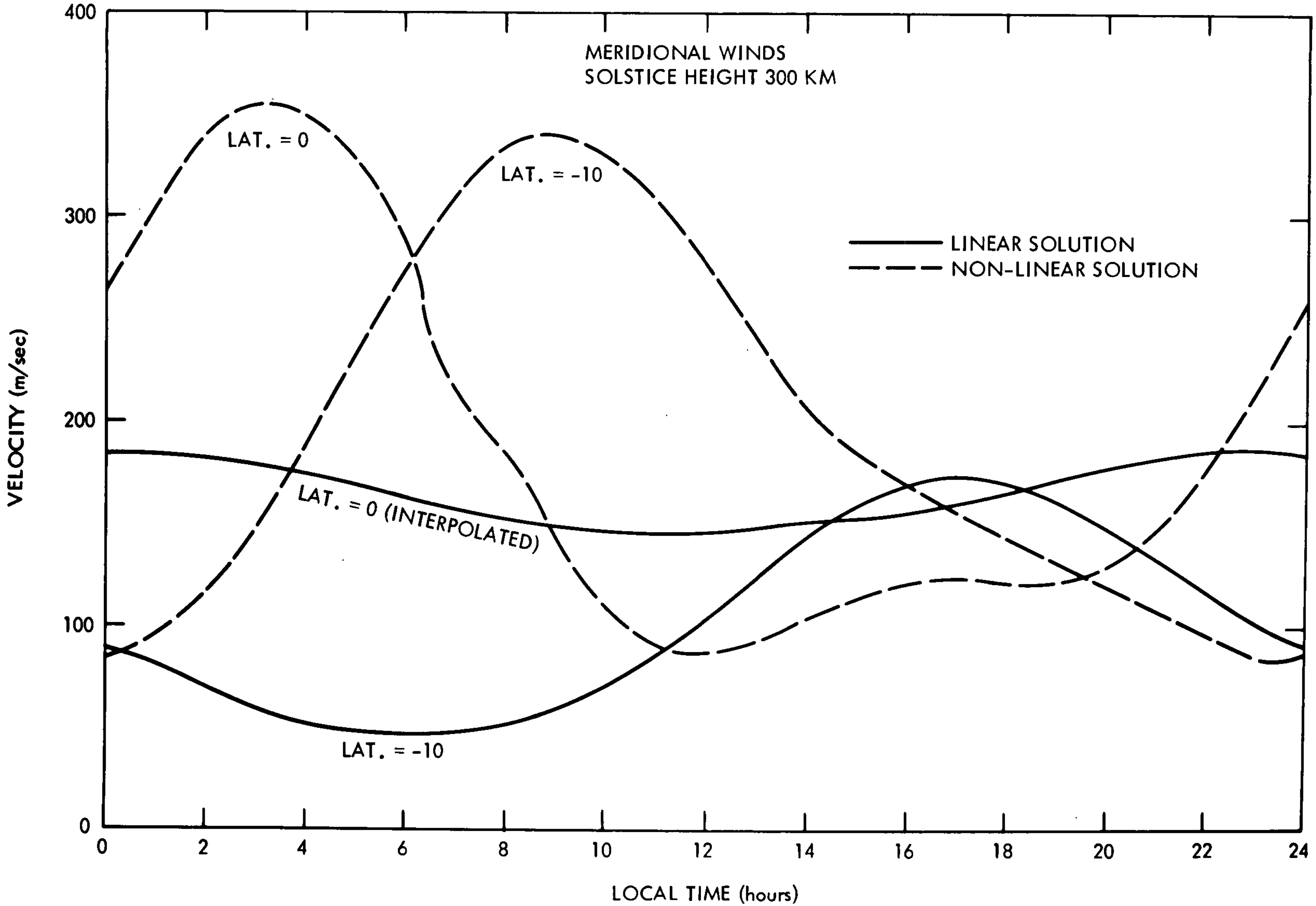
MERIDIONAL WINDS
SOLSTICE HEIGHT 300 KM
LINEAR SOLUTION
NON-LINEAR SOLUTION
LAT. = 0
LAT. = -10
LAT. = 0 (INTERPOLATED)
LAT. = -10
VELOCITY (m/sec)
LOCAL TIME (hours)
0
100
200
300
400
0
2
4
6
8
10
12
14
16
18
20
22
24

Fig. 15

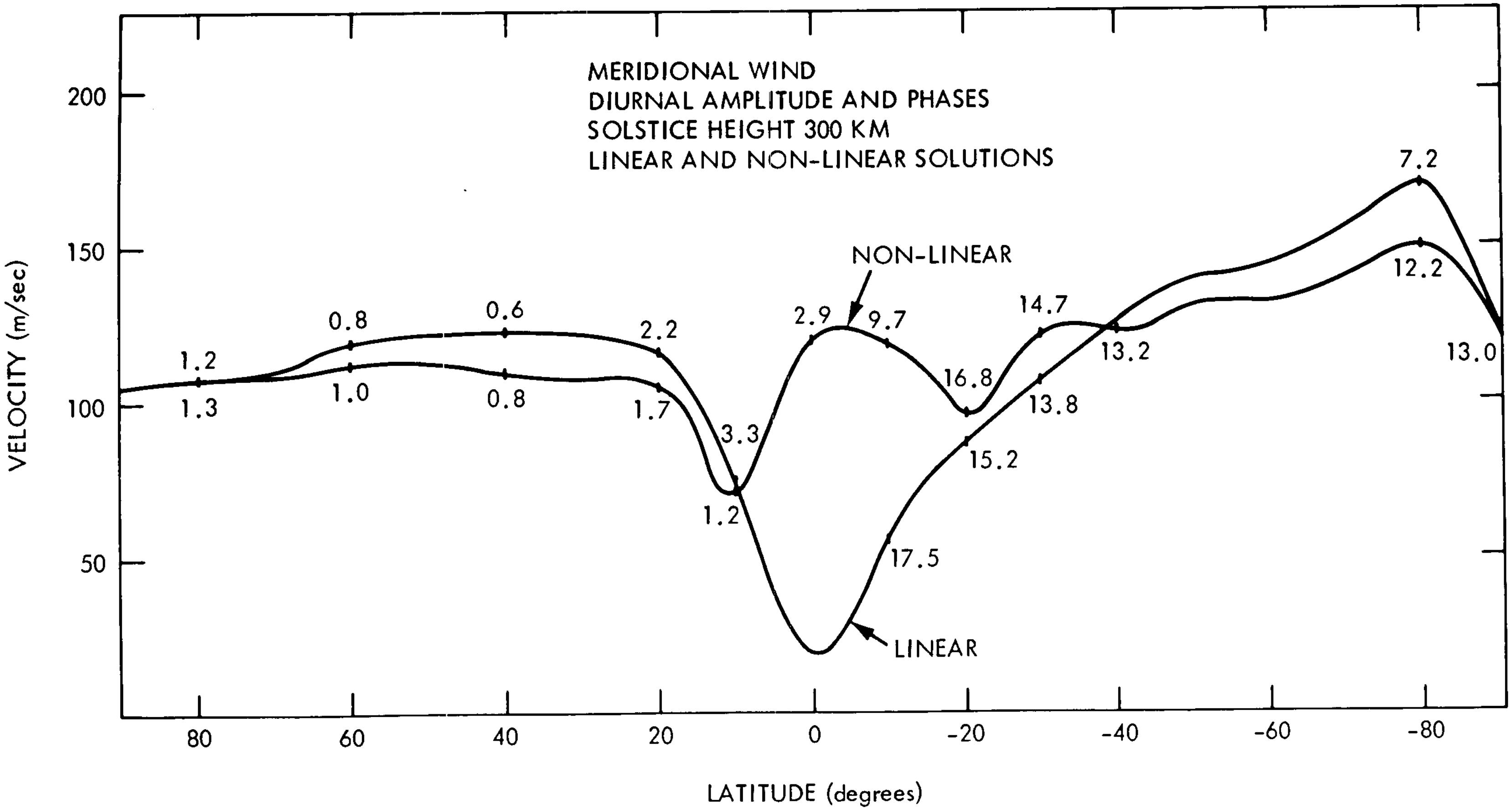

MERIDIONAL WIND
DIURNAL AMPLITUDE AND PHASES
SOLSTICE HEIGHT 300 KM
LINEAR AND NON-LINEAR SOLUTIONS
NON-LINEAR
LINEAR
VELOCITY (m/sec)
LATITUDE (degrees)
200
150
100
50
80
60
40
20
0
-20
-40
-60
-80
1.2
0.8
0.6
2.2
2.9
9.7
14.7
16.8
7.2
12.2
13.0
13.2
13.8
15.2
17.5
3.3
1.2
1.7
0.8
1.0
1.3

Fig. 16

AVERAGE MERIDIONAL VELOCITY
EFFECT OF VISCOCITY
SOLSTICE LAT -10°

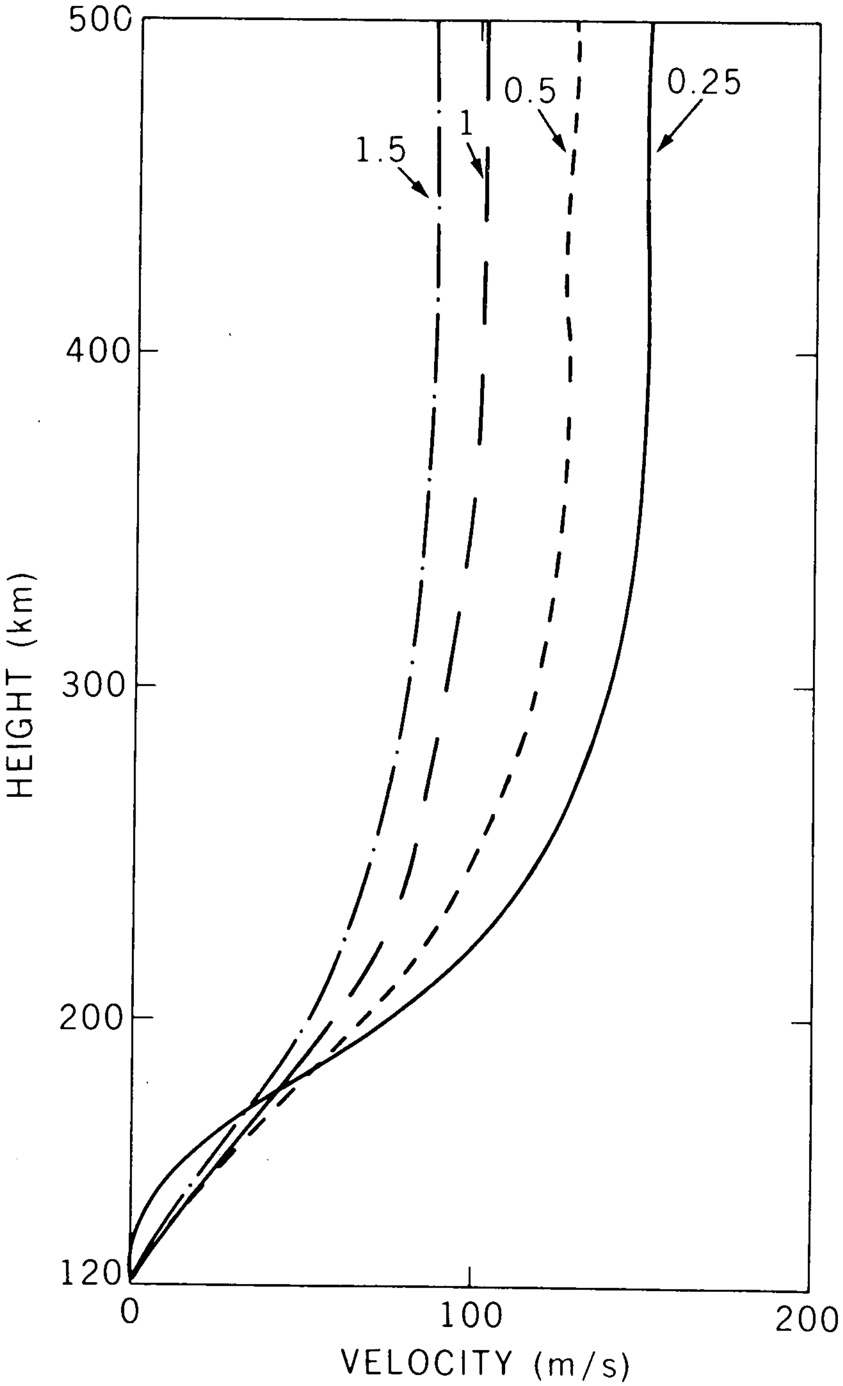

Fig. 17

MID LATITUDE MERIDIONAL WINDS
COMPARISON OF THEORETICAL
CALCULATIONS

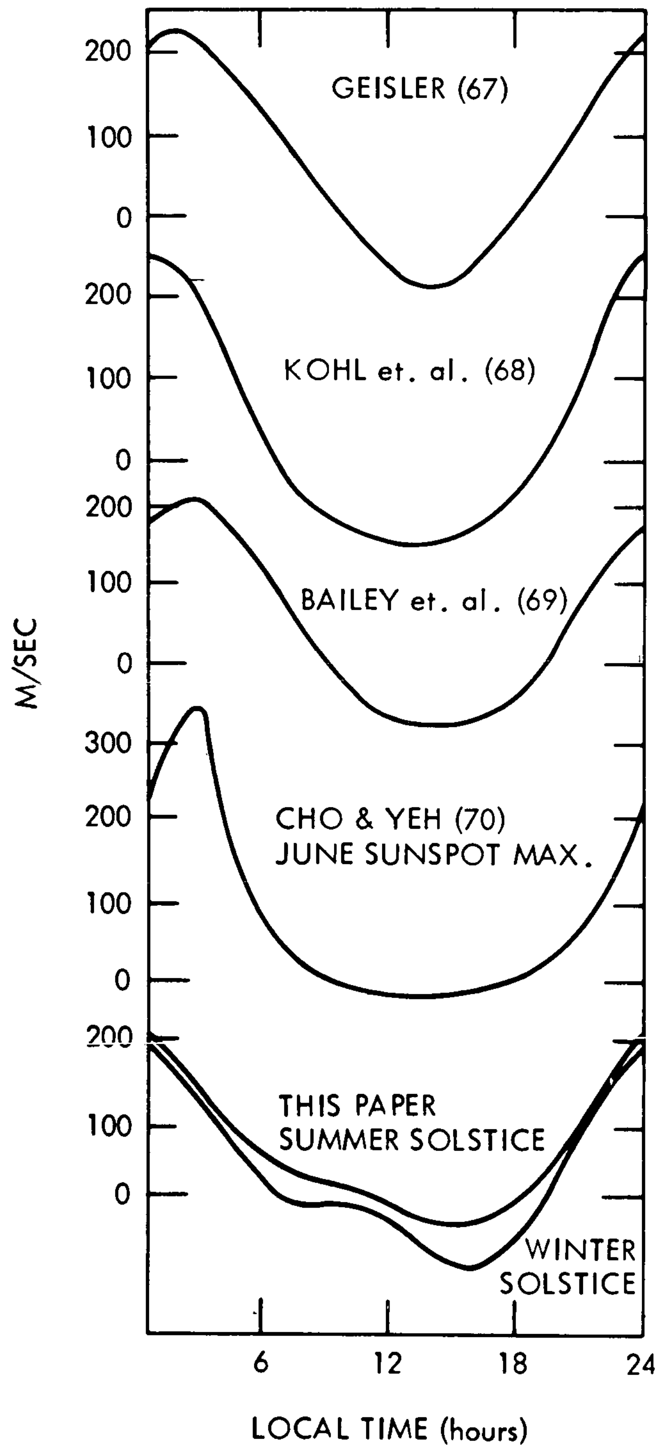

Fig. 18

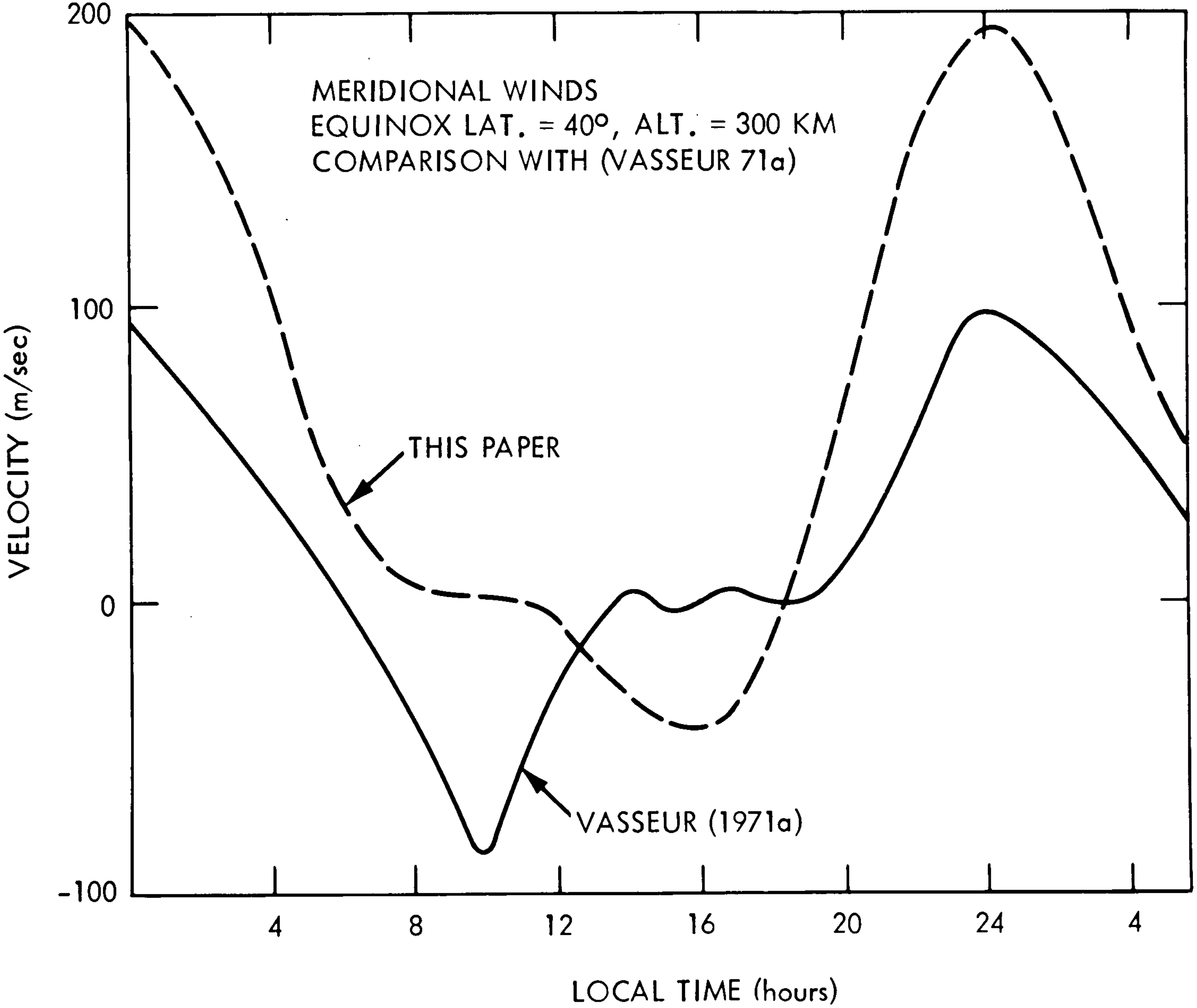
200
100
0
-100
VELOCITY (m/sec)
MERIDIONAL WINDS
EQUINOX LAT. = 40°, ALT. = 300 KM
COMPARISON WITH (VASSEUR 71a)
THIS PAPER
VASSEUR (1971a)
4
8
12
16
20
24
4
LOCAL TIME (hours)

Fig. 19

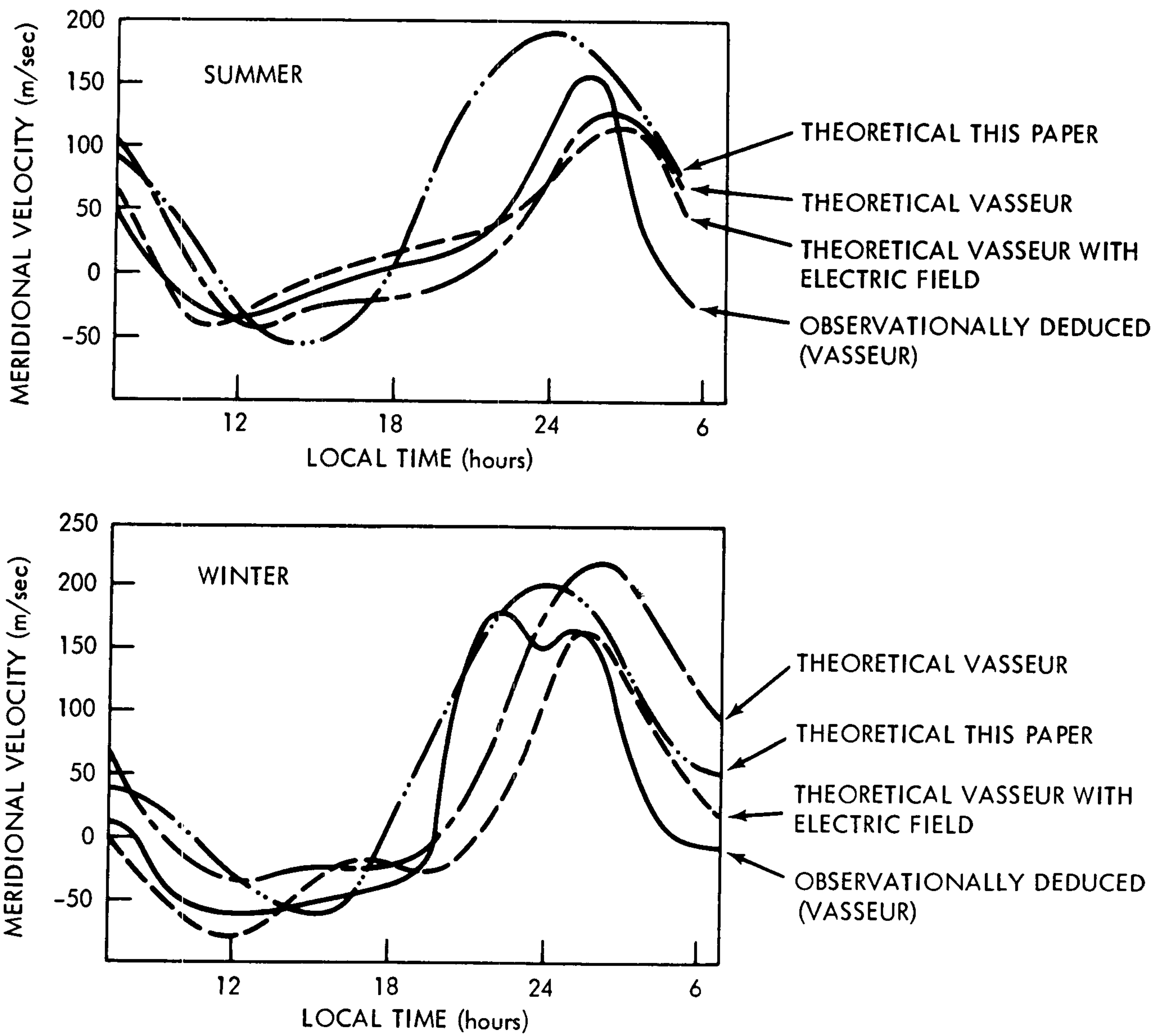
SUMMER
MERIDIONAL VELOCITY (m/sec)
200
150
100
50
0
-50
12
18
24
6
LOCAL TIME (hours)
THEORETICAL THIS PAPER
THEORETICAL VASSEUR
THEORETICAL VASSEUR WITH ELECTRIC FIELD
OBSERVATIONALLY DEDUCED (VASSEUR)
WINTER
MERIDIONAL VELOCITY (m/sec)
250
200
150
100
50
0
-50
12
18
24
6
LOCAL TIME (hours)
THEORETICAL VASSEUR
THEORETICAL THIS PAPER
THEORETICAL VASSEUR WITH ELECTRIC FIELD
OBSERVATIONALLY DEDUCED (VASSEUR)

Fig. 20

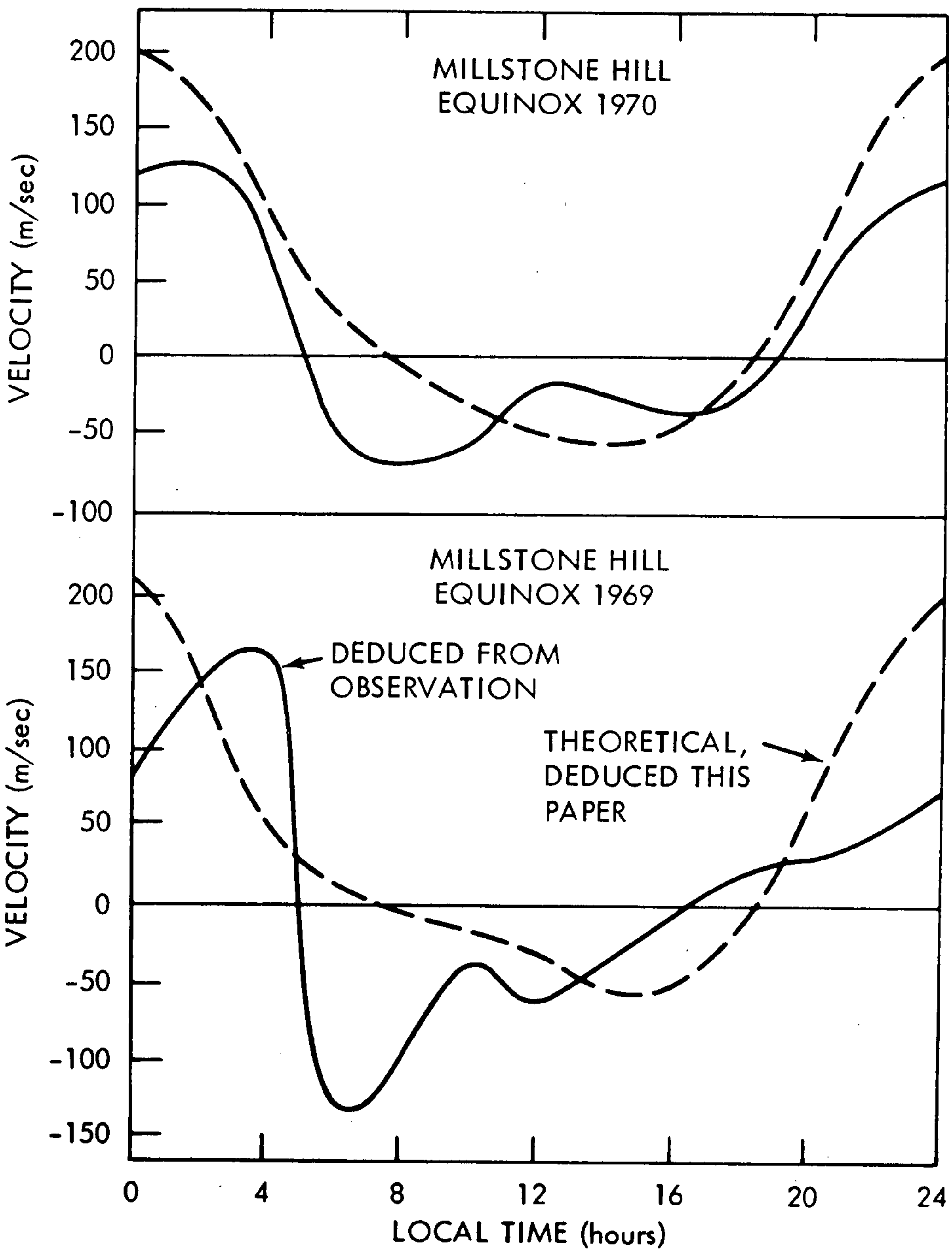
MILLSTONE HILL
EQUINOX 1970
VELOCITY (m/sec)
200
150
100
50
0
-50
-100
MILLSTONE HILL
EQUINOX 1969
DEDUCED FROM
OBSERVATION
THEORETICAL,
DEDUCED THIS
PAPER
VELOCITY (m/sec)
200
150
100
50
0
-50
-100
-150
0
4
8
12
16
20
24
LOCAL TIME (hours)

Fig. 21

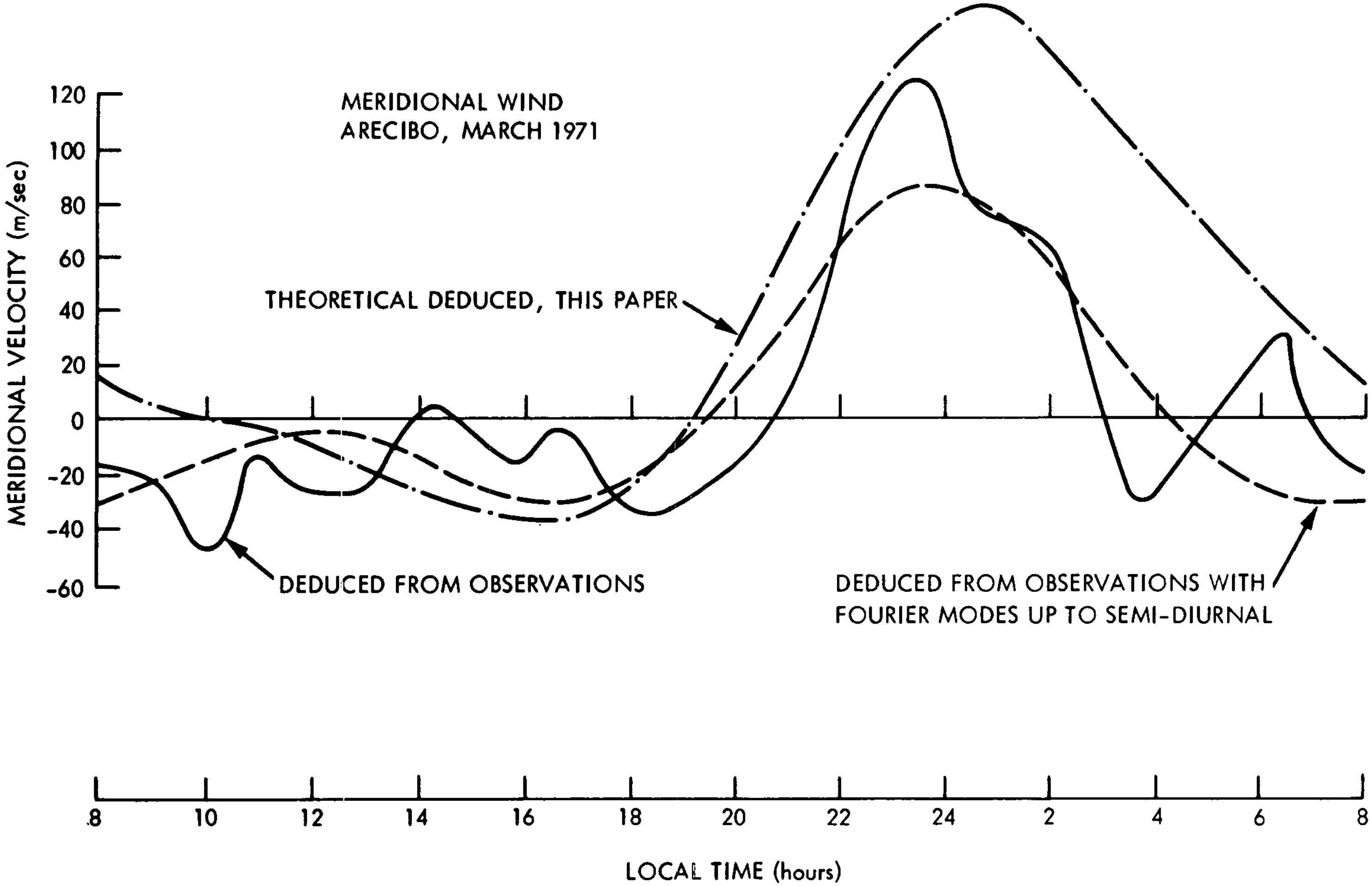
MERIDIONAL WIND
ARECIBO, MARCH 1971
MERIDIONAL VELOCITY (m/sec)
120
100
80
60
40
20
0
-20
-40
-60
THEORETICAL DEDUCED, THIS PAPER
DEDUCED FROM OBSERVATIONS
DEDUCED FROM OBSERVATIONS WITH
FOURIER MODES UP TO SEMI-DIURNAL
8
10
12
14
16
18
20
22
24
2
4
6
8
LOCAL TIME (hours)
Fig. 22

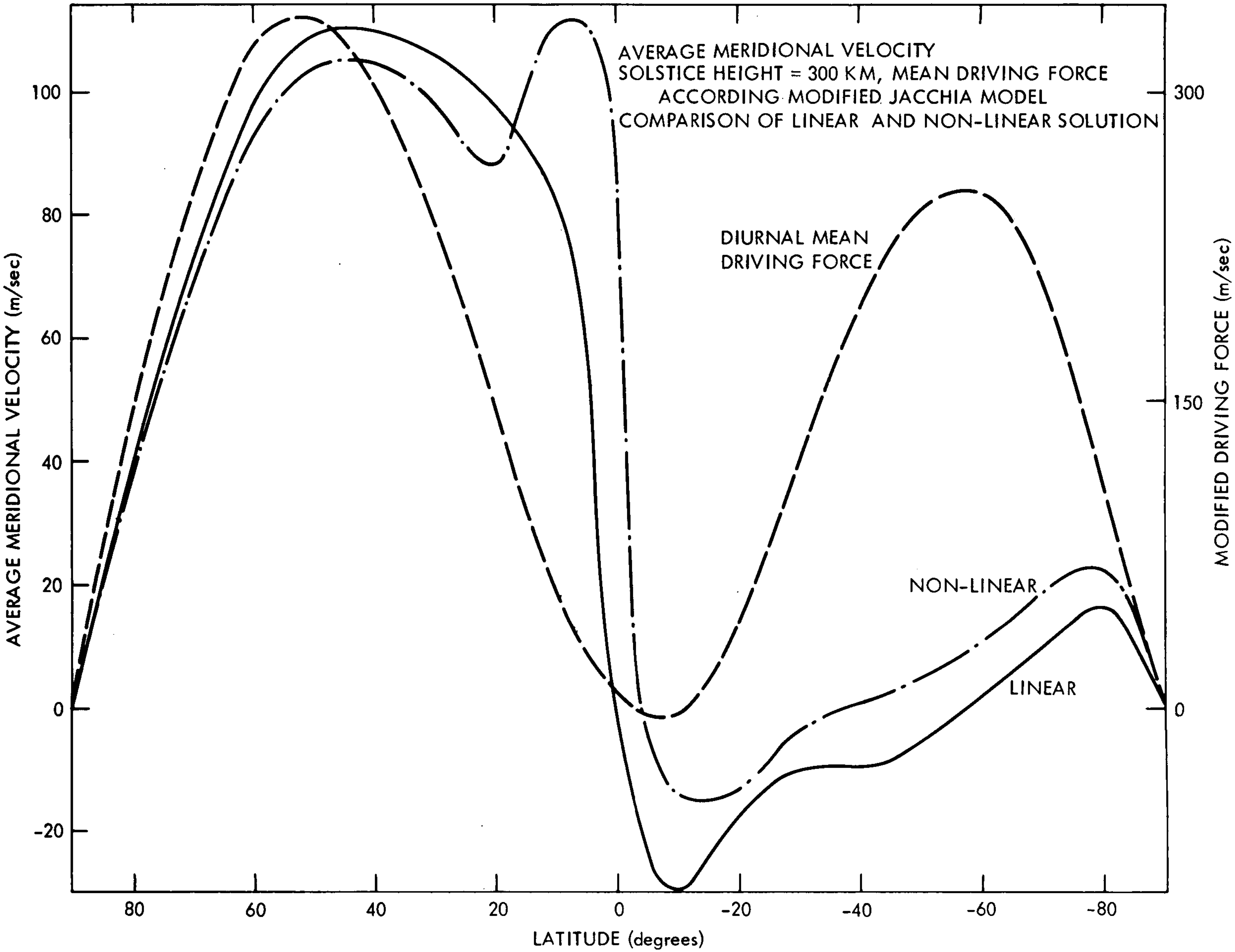
AVERAGE MERIDIONAL VELOCITY
SOLSTICE HEIGHT = 300 KM, MEAN DRIVING FORCE
ACCORDING MODIFIED JACCHIA MODEL
COMPARISON OF LINEAR AND NON-LINEAR SOLUTION
DIURNAL MEAN
DRIVING FORCE
NON-LINEAR
LINEAR
AVERAGE MERIDIONAL VELOCITY (m/sec)
MODIFIED DRIVING FORCE (m/sec)
LATITUDE (degrees)
100
80
60
40
20
0
-20
300
150
0
80
60
40
20
0
-20
-40
-60
-80

Fig. 23

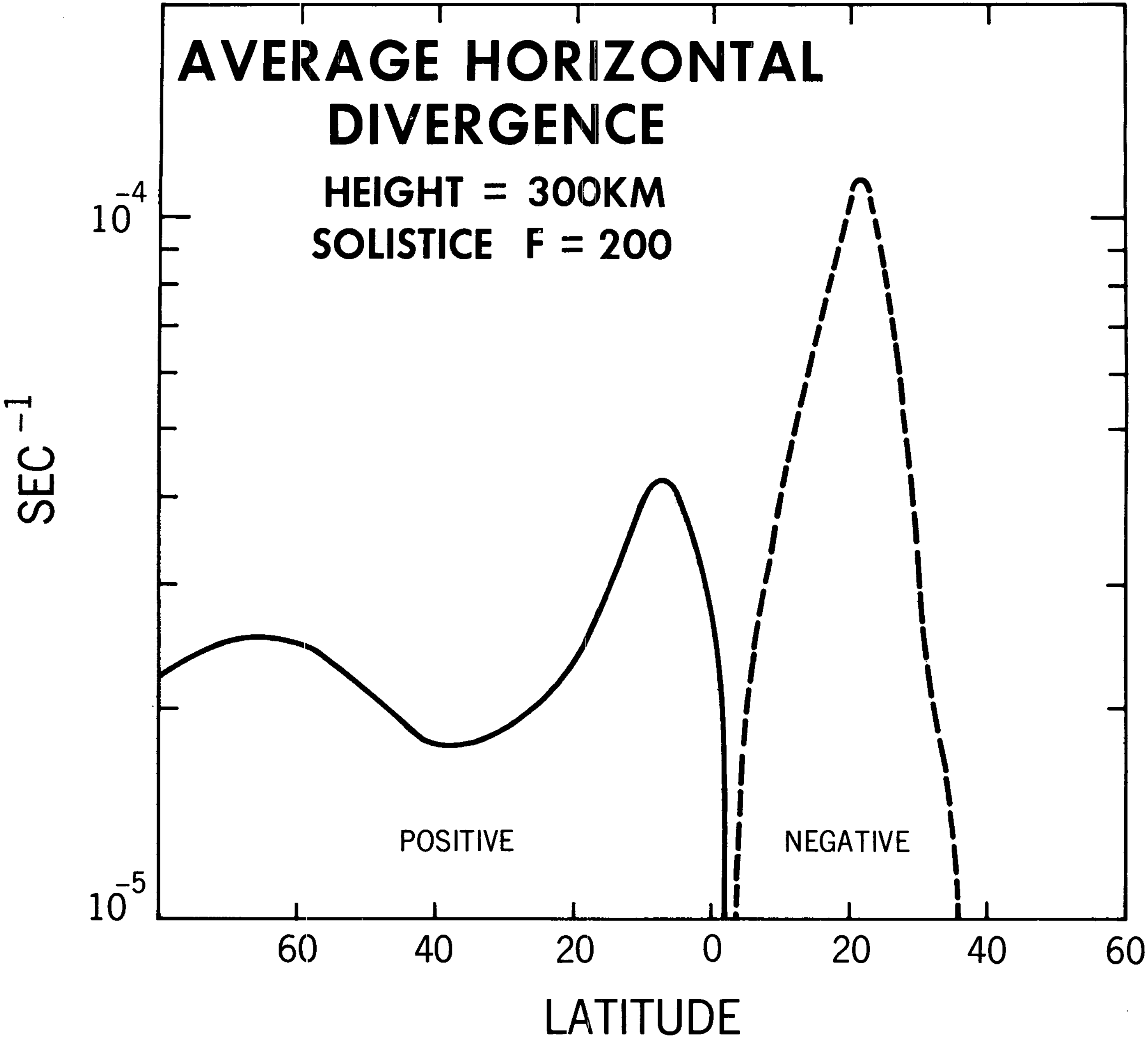
AVERAGE HORIZONTAL DIVERGENCE
HEIGHT = 300KM
SOLISTICE F = 200
10^{-4}
10^{-5}
SEC $^{-1}$
POSITIVE
NEGATIVE
60
40
20
0
20
40
60
LATITUDE

Fig. 24

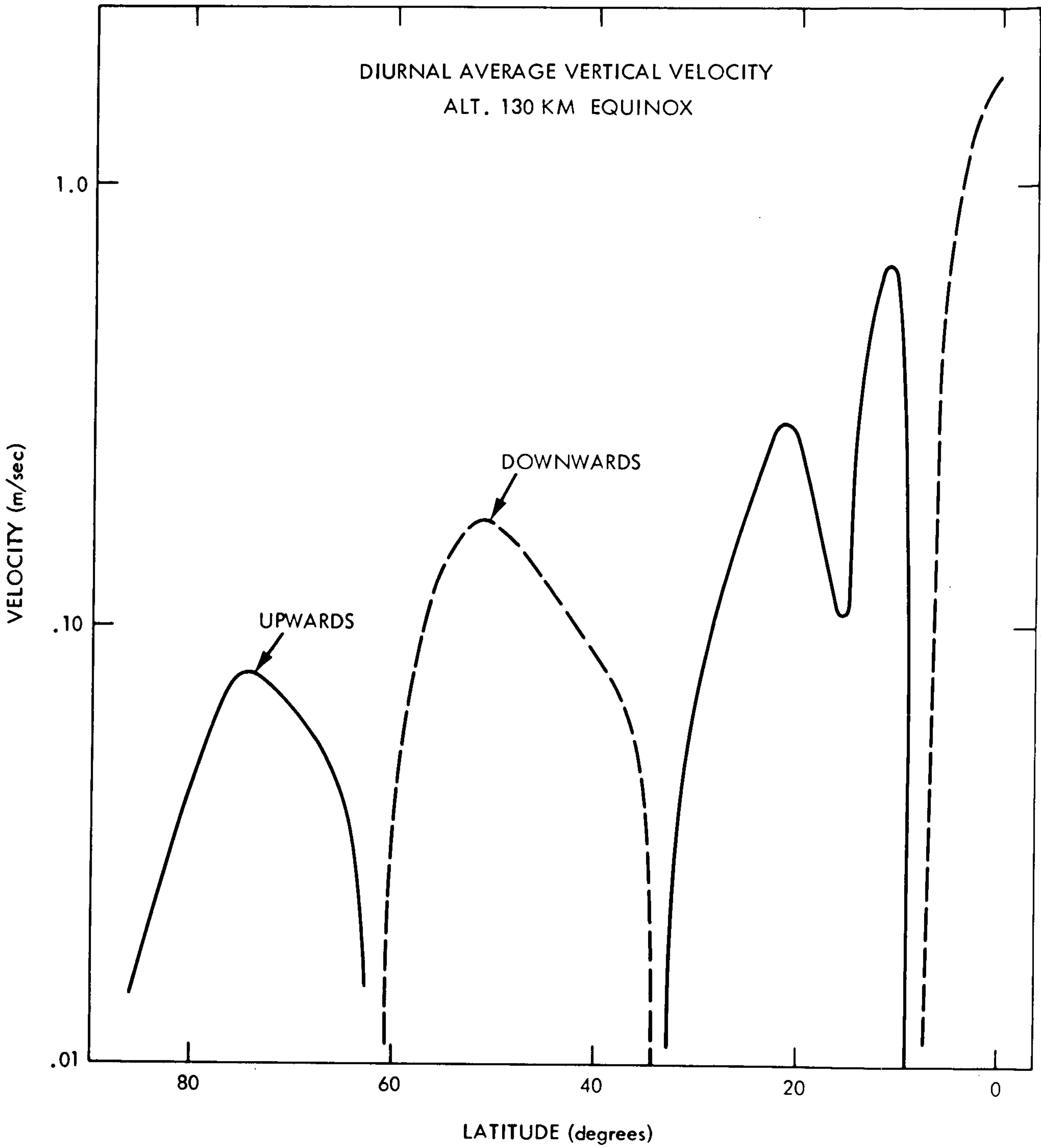
DIURNAL AVERAGE VERTICAL VELOCITY
ALT. 130 KM EQUINOX
VELOCITY (m/sec)
1.0
.10
.01
UPWARDS
DOWNWARDS
80
60
40
20
0
LATITUDE (degrees)

Fig. 25

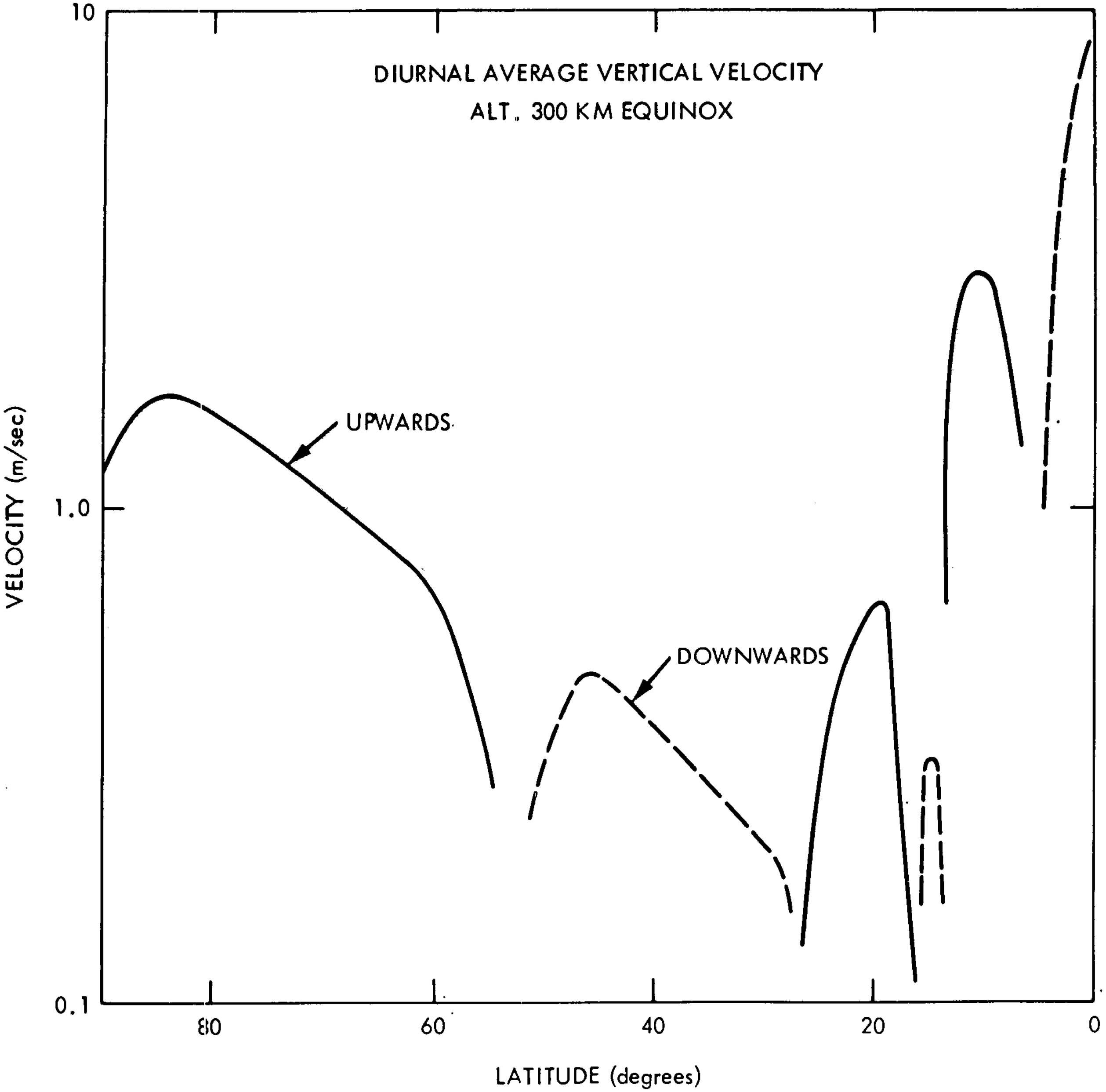
DIURNAL AVERAGE VERTICAL VELOCITY
ALT. 300 KM EQUINOX
UPWARDS
DOWNWARDS
VELOCITY (m/sec)
10
1.0
0.1
80
60
40
20
0
LATITUDE (degrees)

Fig. 25b

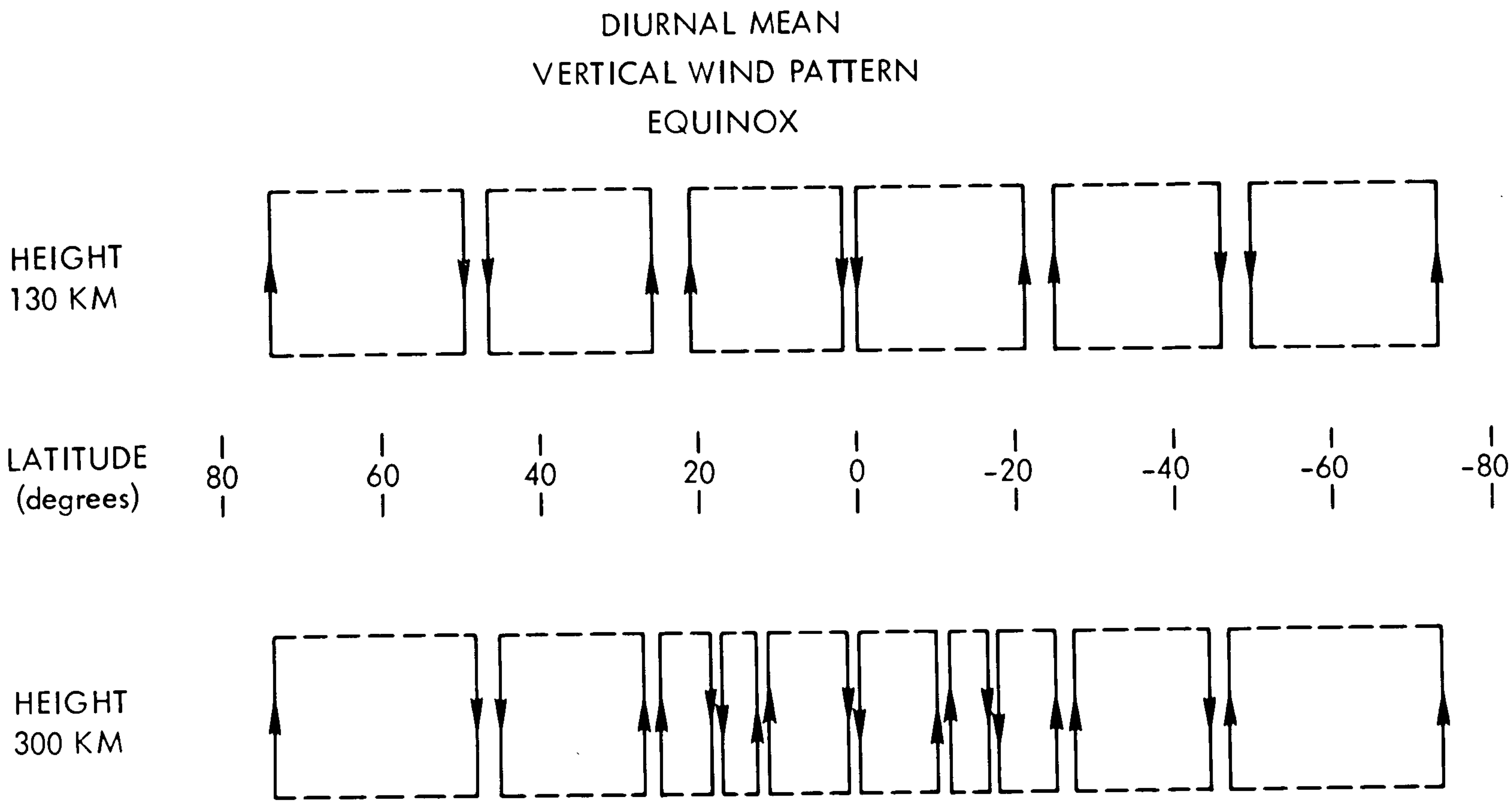
DIURNAL MEAN
VERTICAL WIND PATTERN
EQUINOX
HEIGHT
130 KM
LATITUDE
(degrees)
80
60
40
20
0
-20
-40
-60
-80
HEIGHT
300 KM

Fig. 26

AMPLITUDE OF DIURNAL COMP OF MERIDIONAL VELOCITY EFFECT OF ION DRAG EQUINOX LAT 30°

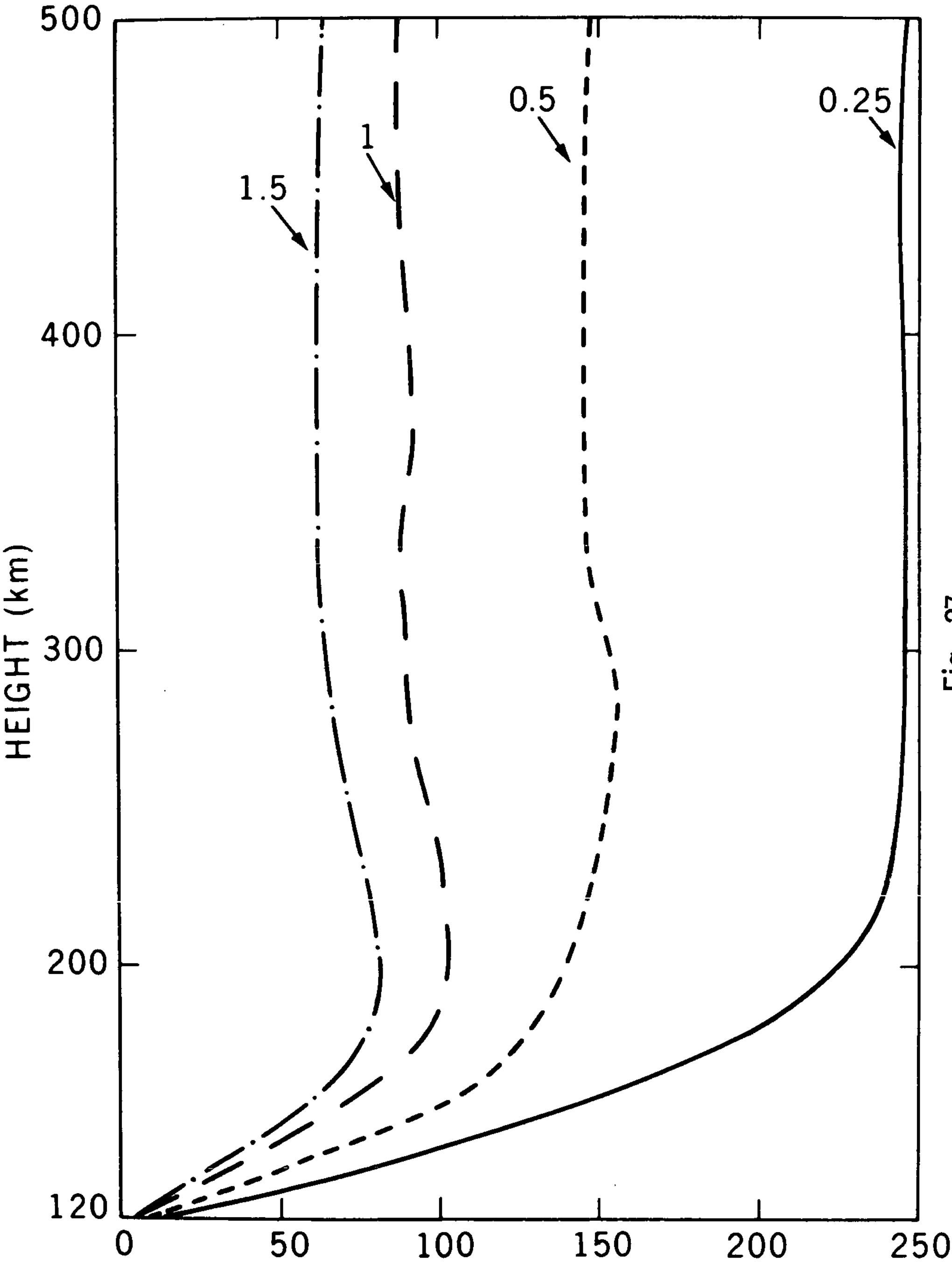

Fig. 27

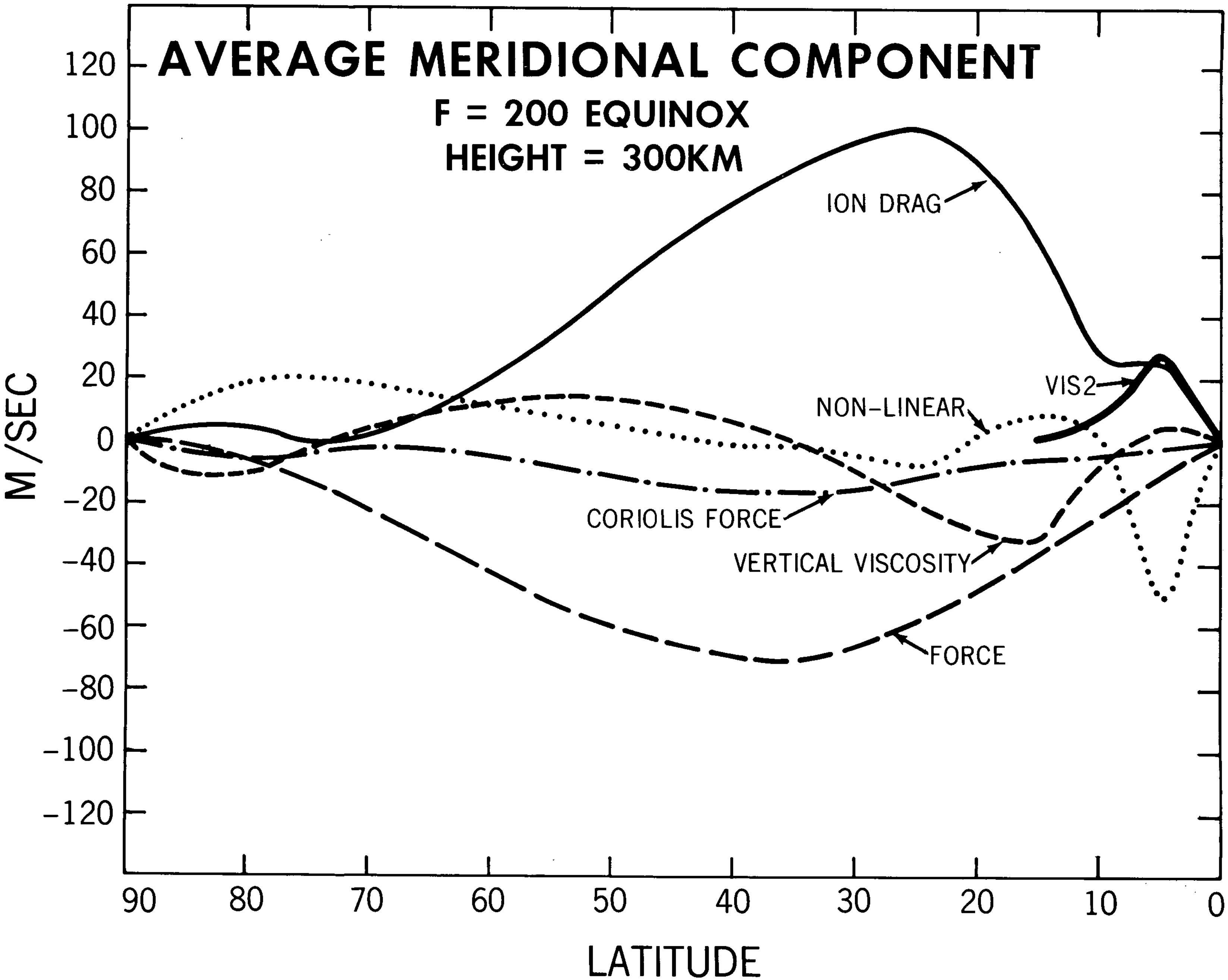
AVERAGE MERIDIONAL COMPONENT
F = 200 EQUINOX
HEIGHT = 300KM
ION DRAG
VIS2
NON-LINEAR
CORIOLIS FORCE
VERTICAL VISCOSITY
FORCE
M/SEC
120
100
80
60
40
20
0
−20
−40
−60
−80
−100
−120
90
80
70
60
50
40
30
20
10
0
LATITUDE

Fig. 28

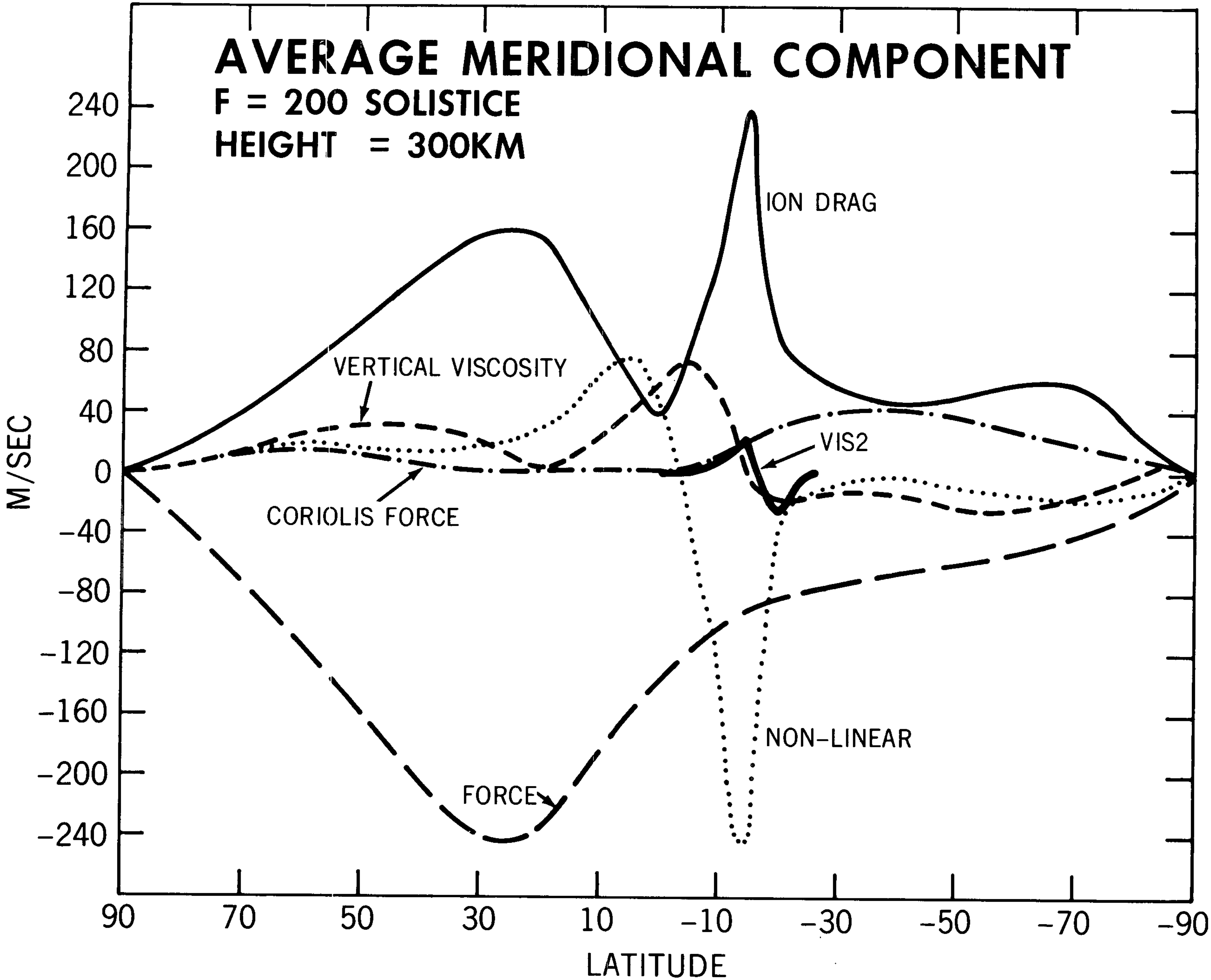
AVERAGE MERIDIONAL COMPONENT
F = 200 SOLISTICE
HEIGHT = 300KM
240
200
160
120
80
40
0
−40
−80
−120
−160
−200
−240
M/SEC
ION DRAG
VERTICAL VISCOSITY
VIS2
CORIOLIS FORCE
NON-LINEAR
FORCE
90
70
50
30
10
−10
−30
−50
−70
−90
LATITUDE
Fig. 29

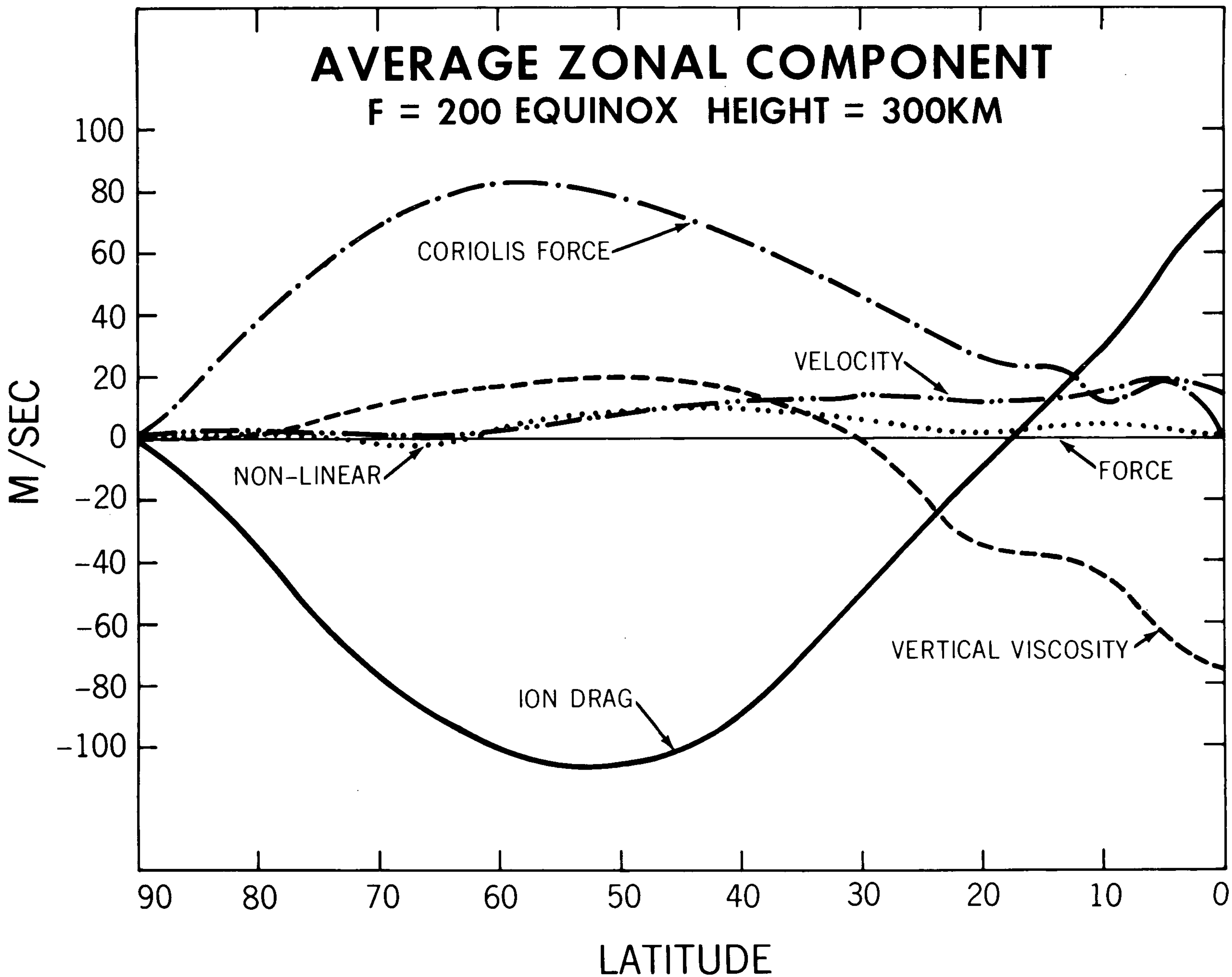
AVERAGE ZONAL COMPONENT
F = 200 EQUINOX HEIGHT = 300KM
M/SEC
100
80
60
40
20
0
-20
-40
-60
-80
-100
CORIOLIS FORCE
VELOCITY
NON-LINEAR
FORCE
VERTICAL VISCOSITY
ION DRAG
90
80
70
60
50
40
30
20
10
0
LATITUDE

Fig. 30

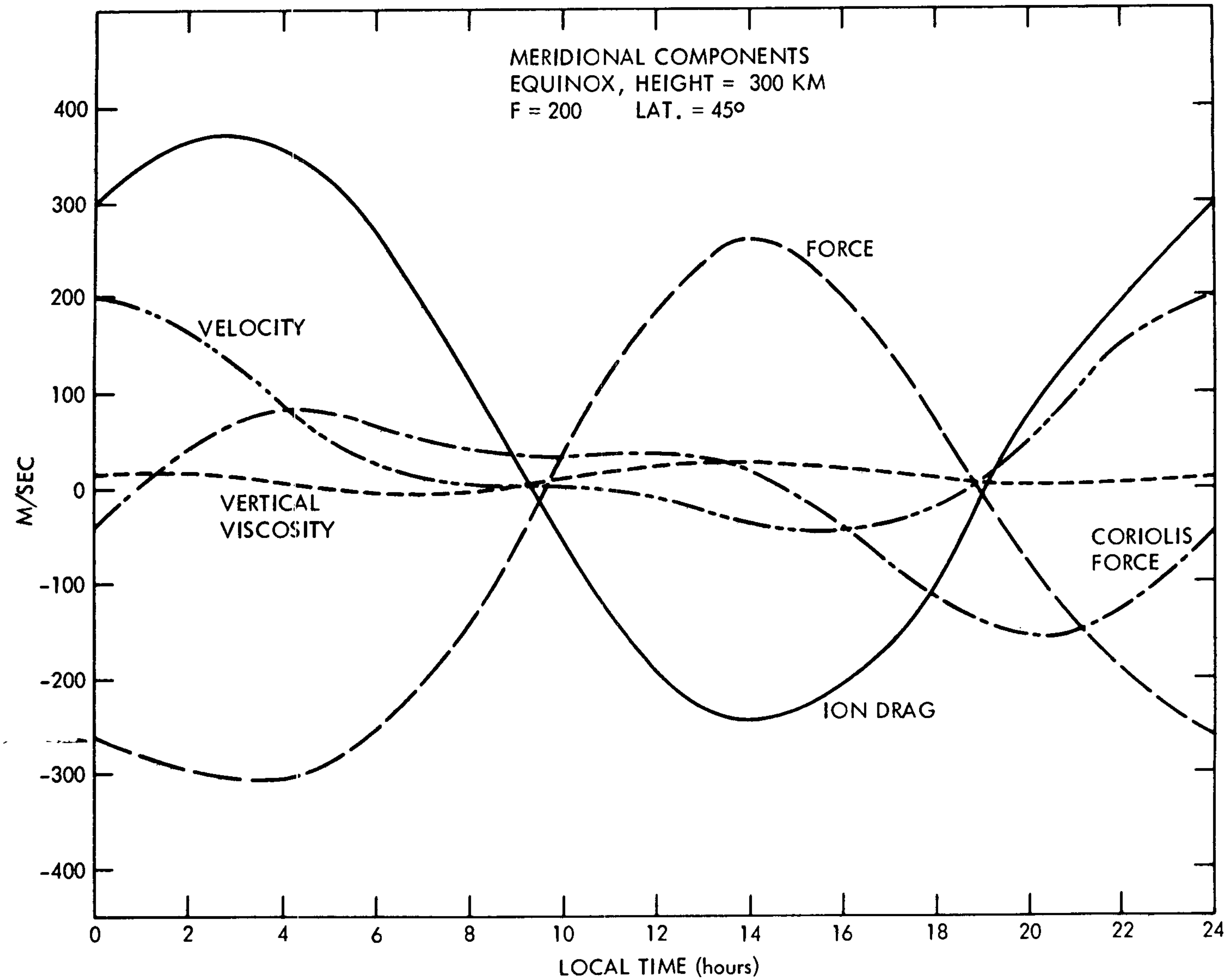

MERIDIONAL COMPONENTS
EQUINOX, HEIGHT = 300 KM
F = 200 LAT. = 45°
FORCE
VELOCITY
VERTICAL
VISCOSITY
CORIOLIS
FORCE
ION DRAG
M/SEC
400
300
200
100
0
-100
-200
-300
-400
0
2
4
6
8
10
12
14
16
18
20
22
24
LOCAL TIME (hours)

Fig. 31

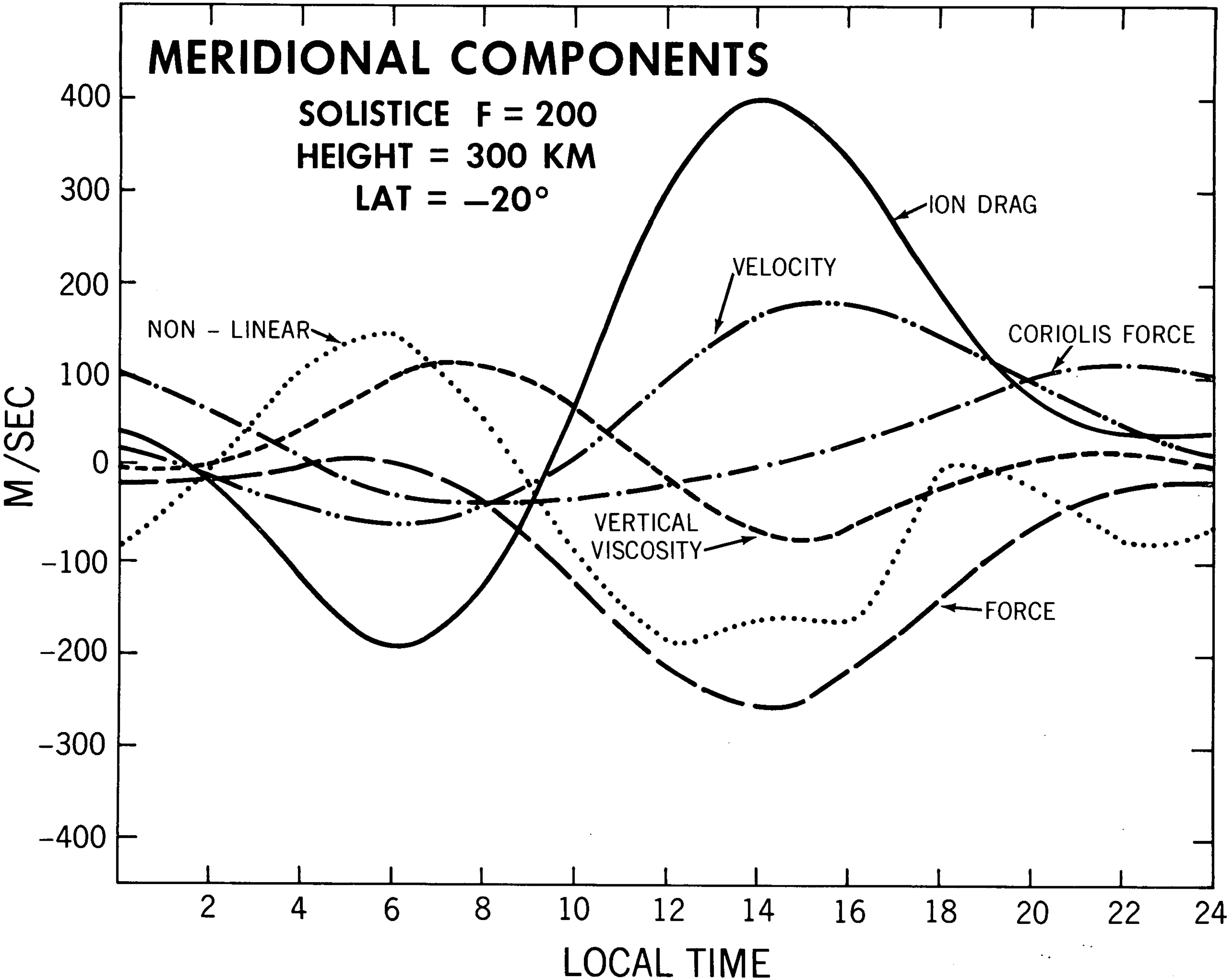
MERIDIONAL COMPONENTS
SOLISTICE F = 200
HEIGHT = 300 KM
LAT = –20°
ION DRAG
VELOCITY
NON – LINEAR
CORIOLIS FORCE
VERTICAL VISCOSITY
FORCE
M/SEC
400
300
200
100
0
–100
–200
–300
–400
2
4
6
8
10
12
14
16
18
20
22
24
LOCAL TIME
Fig. 32